

AD _____

Award Number: W81XWH-10-1-0700

TITLE: Development of a Vaccine Targeting Triple-Negative Breast Cancer

PRINCIPAL INVESTIGATOR: Denise Cecil, Ph.D.

CONTRACTING ORGANIZATION: University of Washington
Seattle, WA 98195

REPORT DATE: November 2013

TYPE OF REPORT: Annual Summary

PREPARED FOR: U.S. Army Medical Research and Materiel Command
Fort Detrick, Maryland 21702-5012

DISTRIBUTION STATEMENT: Approved for Public Release;
Distribution Unlimited

The views, opinions and/or findings contained in this report are those of the author(s) and should not be construed as an official Department of the Army position, policy or decision unless so designated by other documentation.

REPORT DOCUMENTATION PAGE

*Form Approved
OMB No. 0704-0188*

Public reporting burden for this collection of information is estimated to average 1 hour per response, including the time for reviewing instructions, searching existing data sources, gathering and maintaining the data needed, and completing and reviewing this collection of information. Send comments regarding this burden estimate or any other aspect of this collection of information, including suggestions for reducing this burden to Department of Defense, Washington Headquarters Services, Directorate for Information Operations and Reports (0704-0188), 1215 Jefferson Davis Highway, Suite 1204, Arlington, VA 22202-4302. Respondents should be aware that notwithstanding any other provision of law, no person shall be subject to any penalty for failing to comply with a collection of information if it does not display a currently valid OMB control number. PLEASE DO NOT RETURN YOUR FORM TO THE ABOVE ADDRESS.

1. REPORT DATE November 2013			2. REPORT TYPE Annual Summary		3. DATES COVERED 1 September 2010 – 31 August 2013	
4. TITLE AND SUBTITLE Development of a Vaccine Targeting Triple-Negative Breast Cancer			5a. CONTRACT NUMBER			
			5b. GRANT NUMBER W81XWH-10-1-0700			
			5c. PROGRAM ELEMENT NUMBER			
6. AUTHOR(S) Denise Cecil, Ph.D. E-Mail: dcecil@uw.edu			5d. PROJECT NUMBER			
			5e. TASK NUMBER			
			5f. WORK UNIT NUMBER			
7. PERFORMING ORGANIZATION NAME(S) AND ADDRESS(ES) University of Washington Seattle, WA 98195			8. PERFORMING ORGANIZATION REPORT NUMBER			
9. SPONSORING / MONITORING AGENCY NAME(S) AND ADDRESS(ES) U.S. Army Medical Research and Materiel Command Fort Detrick, Maryland 21702-5012			10. SPONSOR/MONITOR'S ACRONYM(S)			
			11. SPONSOR/MONITOR'S REPORT NUMBER(S)			
12. DISTRIBUTION / AVAILABILITY STATEMENT Approved for Public Release; Distribution Unlimited						
13. SUPPLEMENTARY NOTES						
14. ABSTRACT The insulin-like growth factor (IGF) pathway plays an important role in breast cancer growth and metastasis. The IGF-I receptor (IGF-IR) is over-expressed in almost 50% of triple negative breast cancers (TNBC) and is associated with poor prognosis and drug resistance. Thus, therapeutically targeting tumor cells which have upregulated IGF-IR may be a promising approach to treat TNBC. We report that IGF-IR is immunogenic. No toxicities were associated with vaccination targeting IGFIR. Through vaccination, high levels of IGF-IR-specific Th1 could be generated which elicited IFN-g-dependent breast cancer inhibition. SOCS1, upregulated by IFN-g, bound IGF-IR. This interaction inhibited receptor signaling, modulated additional oncogenic proteins, and increased PTEN expression. Oncogenic shock, induced by immunization, restored sensitivity to Tamoxifen therapy in mice refractory to treatment. Cytokine-mediated oncogenic shock may be a mechanism by which cancer vaccines, or other immunotherapies, improve response to subsequent standard treatments resulting in a survival benefit in cancer patients treated with immune modulatory approaches.						
15. SUBJECT TERMS Immunotherapy, IGF-IR, oncogene addiction						
16. SECURITY CLASSIFICATION OF:			17. LIMITATION OF ABSTRACT UU	18. NUMBER OF PAGES 29	19a. NAME OF RESPONSIBLE PERSON USAMRMC	
a. REPORT U	b. ABSTRACT U	c. THIS PAGE U			19b. TELEPHONE NUMBER (include area code)	

TABLE OF CONTENTS

	Page
<u>INTRODUCTION</u>	4
<u>BODY</u>	4
<u>KEY RESERCH ACCOMPLISHEMENTS</u>	10
<u>REPORTABLE OUTCOMES</u>	11
<u>CONCLUSION</u>	11
<u>REFERENCES</u>	12
<u>APPENDICIES</u>	14

INTRODUCTION

The insulin-like growth factor (IGF) pathway plays an important role in breast cancer growth and metastasis. The IGF-I receptor (IGF-IR) is overexpressed in almost 50% of triple negative breast cancers (TNBC), defined as estrogen (ER) and progesterone (PR) receptor and HER-2/neu receptor (HER2) negative. We have determined that IGF-IR is immunogenic in breast cancer and is a potential target for active immunization.

Overexpressed growth factor receptor proteins, including IGF-IR, have been identified as addiction oncogenes in breast cancer as well as other tumors.^{1,2} Tumor cells that have become dependent upon a single activated oncogene for their growth and survival are thought to become oncogene addicted.³ Investigations suggest that oncogene addiction imbalances cell senescent pathways in favor of anti-apoptotic signaling.¹ When a dominant oncogene is acutely inactivated, however, the balance is reversed in favor of pro-apoptotic signaling. The resultant oncogenic shock provides a window of enhanced sensitivity to cell killing prior to addiction developing to other growth or survival signaling pathways.^{4,5}

We hypothesize that immunologic targeting of overexpressed “biologic driver” proteins, those present in oncogenic pathways to which the tumor is addicted,¹ may impart clinical benefit even if induced antigen specific immunity does not completely eradicate the disease. Immune mediated elimination of malignant clones, which have upregulated proteins that confer a growth advantage to the tumor, may result in the development of a cancer remodeled to become a less aggressive variant of the original disease.

The specific aims of this proposal are to: (1) To identify putative Class II epitopes, derived from IGF-IR, that stimulate IGF-IR-specific T cells in patients with breast cancer; (2) To evaluate the immunogenicity, clinical efficacy, and safety of an IGF-IR class II polyepitope vaccine in a mouse model of TNBC.

BODY

Aim 1. To identify putative Class II epitopes, derived from IGF-IR, that stimulate IGF-IR-specific T cells in patients with breast cancer.

Aim 1.a. To identify IGF-IR peptides based on predicted high avidity binding across multiple class II alleles.

The 20 IGF-IR peptides predicted to bind with high affinity to multiple MHC class II alleles are listed in Table 1.^{6,7} The majority of the peptides, 95%, induced significant antigen-specific IFN- γ secretion in both breast cancer and control PBMC (Table 1), as measured by ELISPOT.⁷ Seven percent of donors did not respond to any peptide, 23% of donors responded to 1-3 peptides, 54% of donors responded to 4-10 peptides and 16% of donors responded to >10 peptides. There was no significant difference in the magnitude of response of any individual IGF-IR peptide between patients and controls and both populations had a similar incidence and magnitude of response to CEF peptides ($p=0.357$) (Fig. 1). The CEF peptide pool is derived from cytomegalovirus, Epstein Barr virus and Influenza virus and used here as a positive control.

Since there were no differences between cancer and controls, all 43 donors were considered together for further statistical analyses. The peptides were grouped into domains of IGF-IR. There was a significant increase in the magnitude of response in the C-terminal domain (CTD) compared to the extracellular domain (ECD) ($p<0.001$) or the kinase domain (KD) ($p=0.001$) (Fig 1). Significantly more subjects responded to epitopes in the CTD of the protein (median percent responding: 48%), compared to epitopes in the ECD (median percent responding: 27%; $p=0.035$) (Fig 2).

Table 1. IGF-IR specific Type I T cells are readily detected in the peripheral blood of breast cancer patients and volunteer donors.

	Control		Cancer	
	Mean	Range	Mean	Range
p7-21	11.2	0-63.2	10.4	0-73.3
p24-38	23.8	0-85.8	13.9	0-62.8
p39-53	12.8	0-79.7	20.7	0-65
p76-90	31.8	0-91.3	35.1	0-160
p354-368	14.6	0-92.5	12	0-80.1
p363-377	0		0	
p388-402	9.8	0-54.3	6	0-72
p554-559	4.8	0-46	8.7	0-76.8
p787-801	8.5	0-47.1	6.1	0-49.3
p891-905	33.6	0-126.6	15.8	0-68.8
p906-920	24	0-118.9	20	0-94
p921-935	20.1	0-118	15.6	0-39
p1028-1042	33	0-91.6	20.8	0-93
p1080-1094	7	0-57.8	5.3	0-81.6
p1092-1106	10.4	0-69.8	13	0-101.6
p1166-1180	20.5	0-114	5.5	0-50
p1212-1226	20.3	0-134	10.7	0-85.7
p1302-1316	24.3	0-112.6	22.4	0-81.8
p1307-1321	34.8	0-134.7	29.8	0-97
p1311-1325	34.9	124.3	24.5	0-91

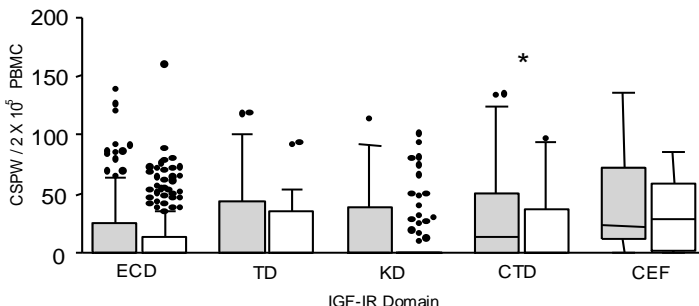


Figure 1. IGF-IR peptides in the CTD induce a higher magnitude of IFN- γ response than the other domains. IFN- γ ELISPOT for volunteer (n=23; gray bars) and breast cancer (n=20; white bars) PBMC for IGF-IR peptides in the extracellular domain (ECD), transmembrane domain (TD), kinase domain (KD), C-terminal domain (CTD) and CEF peptides. The data are presented as interquartile box plots with Tukey whiskers. Median corrected spots per well (CSPW) are indicated by the horizontal bar; *p<0.01 compared to ECD and TM.

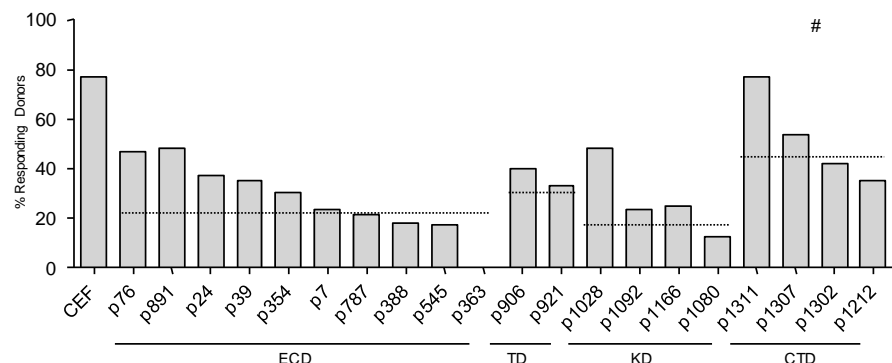
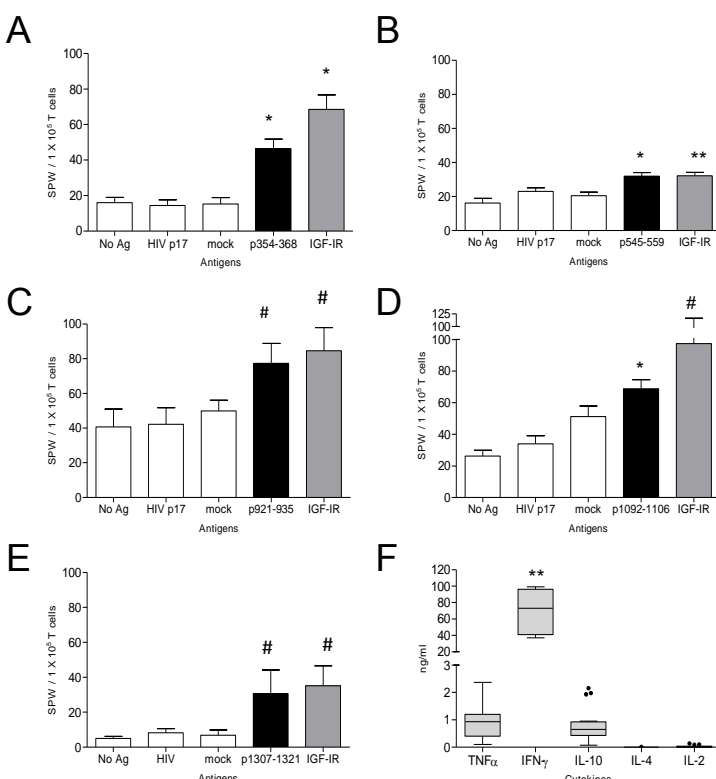


Figure 2. IGF-IR CTD peptides induce IFN- γ secretion in significantly more donors. Horizontal dashed line indicates the median percent responding in each domain; #p<0.05 compared to all other domains.



To determine whether responding peptides were native epitopes of IGF-IR, peptide specific T cell lines were generated from three control and two cancer donor's PBMC and evaluated for specificity to human IGF-IR.⁷ The peptides were randomly chosen, two peptides from the ECD, and one peptide each from the TM, KD and CTD. Each peptide was 100% homologous with murine IGF-IR. The T cell lines (mean, 98.4% CD3 $^{+}$ cells) were predominantly CD4 $^{+}$ (mean, 67.8%; range 59.8-73.6%), with CD8 $^{+}$ (mean, 25.5%; range, 23.3-28.4%) and CD4 $^{-}$ CD8 $^{-}$ (mean, 1.2%; range 0.68-1.88%) cells. The T cell lines generated were both IGF-IR peptide (p354-368, p=0.001; p545-559, p=0.013; p921-935, p=0.041; p1092-1210, p=0.002; p1307-1321, p=0.04 compared to HIV p17) and IGF-IR protein specific (p354-368, p=0.001; p545-559, p=0.001; p921-935, p=0.04; p1092-1210, p=0.03; p1307-1321, p=0.04 compared to mock transfectants) (Fig. 3A-E). All the IGF-IR specific T cell lines secreted Type 1 cytokines; TNF α (mean, 1,028 pg/ml; range 101-2,370 pg/ml) and IFN- γ (mean, 68,419 pg/ml; range, 37,030-99,106 pg/ml). Additionally, the T cell lines secreted the Type 2 cytokine, IL-10 (mean, 823 pg/ml; range 71-2,154 pg/ml). IFN- γ secretion was significantly greater than TNF α (p=0.002) or IL-10 secretion (p=0.003) (Fig. 3F). Minimal IL-2 (mean, 26 pg/ml; range, 0-132 pg/ml) and no IL-4 (mean, 0) was detected.

Aim 1.c. To determine whether identified IGF-IR peptides stimulate T regulatory (Treg) cell proliferation.

Tregs can modulate the immune response by secreting the immunosuppressive cytokines IL-10 and TGF β .^{8,9} Given that Tregs can proliferate in the peripheral blood in response to stimulation with 15-mer peptides specific for common tumor antigens⁹, we identified class II epitopes in IGF-IR that might preferentially enhance the growth of Tregs. IL-10 ELISPOT was performed on 20 volunteer and 20 breast cancer donor PBMC.¹⁰

Figure 3. IGF-IR peptides are native MHCII epitopes. (A-E) IFN- γ ELISPOT for IGF-IR peptide-specific T cell lines. Antigens include IGF-IR peptides, cos-1 cell lysate transfected with pcDNA3 encoding IGF-IR, and HIV p17 and cos-1 lysate transfected with empty pcDNA (mock) are used as negative controls. Data are expressed as mean spots per well \pm SD; **p<0.001, *p<0.01, #p<0.05. (F) Cytokine secretion from IGF-IR T-cell lines pooled from 5 different donors expanded with peptides p354, p545, p921, or p1092; **p<0.001 compared to TNF α and IL-10 secretion.

Similarly to that observed with IFN- γ secretion, there was no significant difference in response between cancer and controls for any individual peptide. Thirty-seven percent of donors did not respond to any peptide, 5% of donors responded to 1-3 peptides, 17% of donors responded to 4-10 peptides and 6% of donors responded to >10 peptides. There was a significant increase in the magnitude of response in the ECD ($p=0.012$), TMD ($p=0.006$) and KD (0.008) compared to the CTD (Fig. 4). Significantly more subjects responded to epitopes in the TD of the protein (median percent responding: 38%), compared to epitopes in the CTD (median percent responding: 15%; $p=0.001$) (Fig 5).

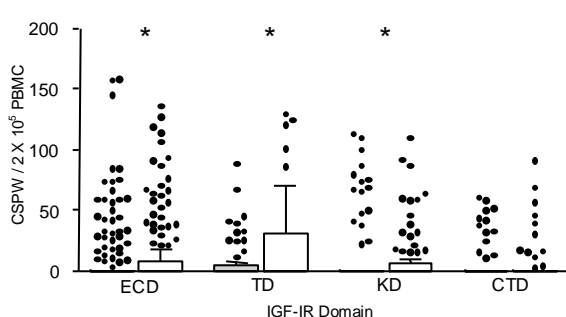


Figure 4. Some IGF-IR peptides are potentially immunosuppressive. IL-10 ELISPOT for volunteer ($n=20$; gray bars) and breast cancer ($n=20$; white bars) in each of the IGF-IR domains. The data are presented as interquartile box plots with Tukey whiskers. Median corrected spots per well (CSPW) are indicated by the horizontal bar; * $p<0.01$ compared to CTD.

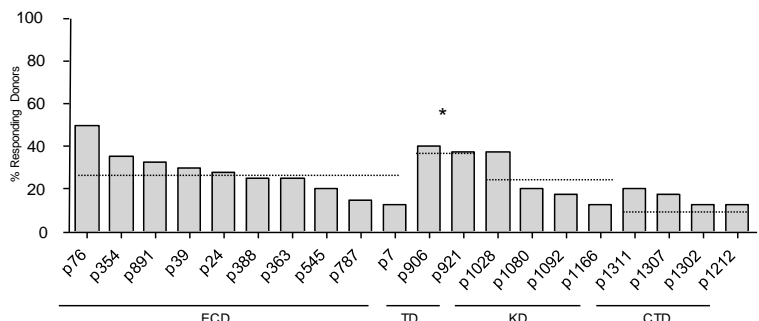


Figure 5. A greater percentage of donors have T cells that secrete IL-10 when stimulated with IGF-IR peptides in the TD. Horizontal dashed line indicates the median percent responding in each domain; * $p<0.01$ compared to CTD.

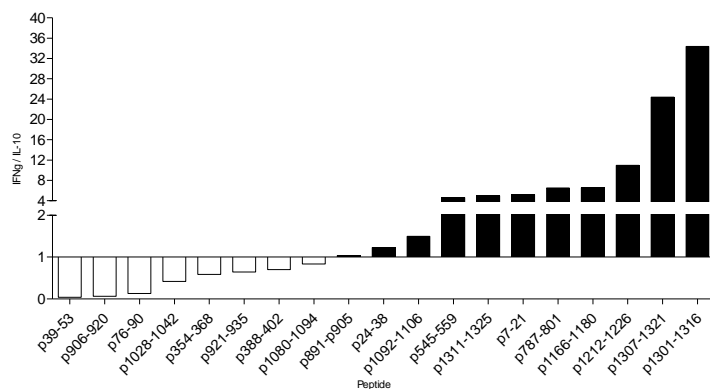


Figure 6. CTD peptides stimulate a Th1 immune response with limited immunosuppression. IGF-IR peptides were analyzed by the magnitude and frequency of response to both IFN- γ and IL-10 ELISPOT in breast cancer donors. Peptides were ranked from preference to secrete IL-10 to preference to secrete IFN- γ . No preference to secrete either cytokine is indicated at 1 on the y-axis.

To choose peptides for the multi-epitope vaccine that induced increased IFN- γ without inducing IL-10, we created a ratio of IFN- γ to IL-10 that analyzed both the magnitude and frequency of ELISPOT response using the following algorithm: corrected mean spots per well \times percent of responding donors. Although there were no differences observed in any individual peptides for both IL-10 and IFN- γ secretion, we used the magnitude and frequency of responses for cancer patients only. The peptides were ranked from highest IL-10 response to highest IFN- γ response, where high IL-10 compared to IFN- γ is shown below 1 and high IFN- γ compared to IL-10 is shown above 1 (Fig 6). The top three peptides (p1301-1316, p1307-1321, and p1212-1226) are in the CTD and the fourth peptide (p1166-1180) is in the kinase domain. These peptides, along with p1311-1325 were chosen for the multi-epitope vaccine. Though not in the top four peptides,

p1311-1325 was chosen to be included

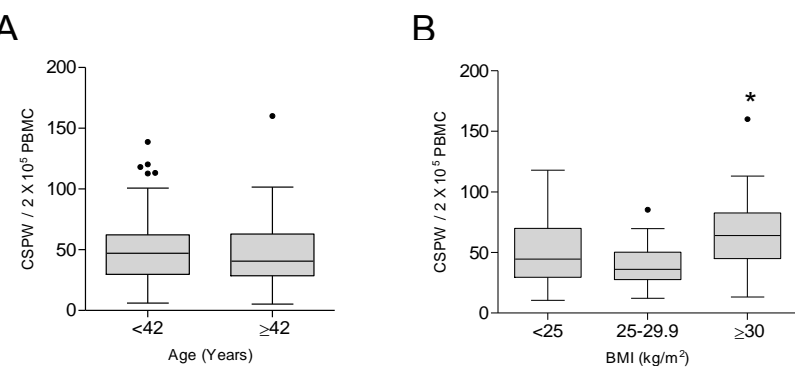


Figure 7. Higher levels of IGF-IR-specific Th1 are found in the peripheral blood of obese as compared to healthy weight and overweight individuals regardless of a breast cancer diagnosis. (A) IFN- γ CSPW for all positive responses according to median age (42 years) presented as interquartile box plots with Tukey whiskers. Median CSPW are indicated by the horizontal bar. (B) IFN- γ CSPW for all positive responses graphed according to BMI. BMI<25 kg/m² (healthy weight); BMI=25.0–29.9 kg/m² (overweight); BMI \geq 30.0 kg/m² (obese). * $p<0.01$.

since it was very similar to p1307-1321 and predominantly induced secretion of IFN- γ .

Th2 immunity appeared to be more prevalent and of higher magnitude in patients with breast cancer, however, IGF-IR-specific Th1 immunity had no such association. We then explored additional factors, known to potentially impact immunity, as a potential etiology for presence of detectable IGF-IR-specific Th1 in both populations. Studies have demonstrated autoantibody levels and autoreactive lymphocytes increase with age in humans and primates¹¹⁻¹³, however, there was no significant difference in the incidence ($p=0.198$) or magnitude ($p=0.223$) (Fig. 7A) of IGF-IR-specific Th1 between donors below the median age of 42 years compared to those donors above the median age. Obesity is marked by elevated levels of circulating CD4 $^{+}$ T-cells secreting IFN- γ .¹⁴ Moreover, IGF-IR has been shown to be aberrantly expressed in obese adipocytes.¹⁵ For this reason, we explored the relationship of the incidence and magnitude of antigen-specific Th1 with Body Mass Index (BMI). There was no significant difference in the incidence of IGF-IR immunity by BMI ($p>0.05$ for all groups), however, we observed a significantly greater magnitude of IGF-IR IFN- γ -secreting T-cells in obese subjects than overweight ($p<0.001$) or healthy weight ($p=0.006$) subjects regardless of a breast cancer diagnosis (Fig. 7B). No significant difference was observed in IL-10 incidence or magnitude when stratified by age ($p=0.174$, $p=0.966$, respectively) or BMI ($p=0.137$, $p=0.174$, respectively).

Aim 2. To evaluate the immunogenicity, clinical efficacy, and safety of an IGF-IR class II polyepitope vaccine in a mouse model of TNBC.

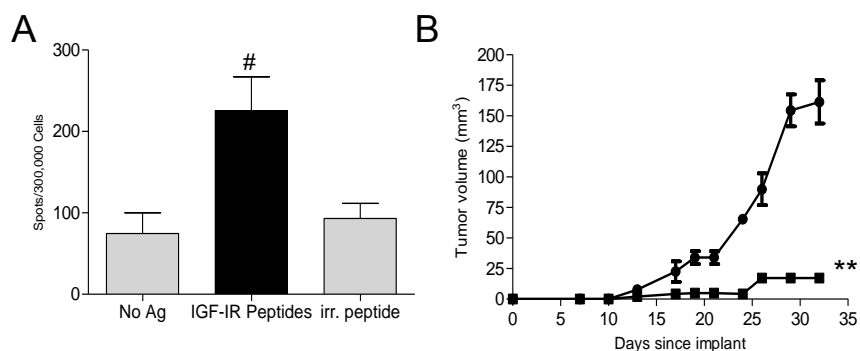


Figure 8. CTD peptides induce a Th1 immune response and inhibit tumor growth in TgC3(I)-Tag mice. (A) IFN- γ ELISPOT from mice vaccinated with the IGF-IR-CTD peptide pool. The antigens include the CTD peptide pool, and irrelevant (irr.) peptide and no antigen (Ag) are used as negative controls ($n=5$); * $p<0.05$ compared to either no Ag or irr. peptide. (B) Mean tumor volume ($\text{mm}^3 \pm \text{SEM}$) from mice injected with PBS alone (●) or IGF-IR vaccine (■) ($n=8$); ** $p=0.001$.

Aim 2.a. To determine the immunogenicity and therapeutic efficacy of IGF-IR immunization.

Breast cancers derived from TgC3(I)-Tag mice express IGF-IR (data not shown). Non-tumor bearing parental FVB/N mice were immunized with IGF-IR-CTD peptide pool (p1301-1316, p1307-1321, p1311-1325 and p1212-1226).⁷ All peptides were 100% homologous to the mouse protein. Antigen specific T cells were generated after vaccination ($p=0.026$ compared to HIV peptide) (Fig. 8A). TgC3(I)-Tag mice were also vaccinated with the IGF-IR-CTD peptide pool. The syngeneic tumor cell line M6¹⁶ was implanted subcutaneously in the flank of the mouse.⁷ After 32 days of growth, the mean tumor volume of the IGF-IR-CTD vaccinated group was $17 \pm 3 \text{ mm}^3$ compared to $161 \pm 17 \text{ mm}^3$

Aim 2.b. To determine which immune effector arm is essential for mediating therapeutic efficacy after immunization.

To assess which T-cell subset mediated the antitumor effect, IGF-IR vaccinated mice were selectively depleted of CD4 $^{+}$ and CD8 $^{+}$ T-cells prior to tumor challenge. B-cells were also depleted as IGF-IR specific antibodies have been shown to mediate tumor regression.¹⁷ IGF-IR vaccination

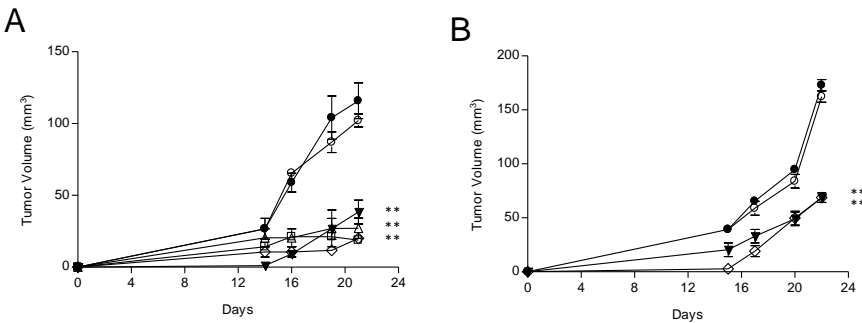


Figure 9. Th1 cells, elicited by IGF-IR vaccination, inhibit the growth of breast cancer via IFN- γ secretion. (A) Mean tumor volume ($\text{mm}^3 \pm \text{SEM}$) from mice injected with adjuvant (●), IGF-IR vaccine (○), or IGF-IR vaccine with isotype control Ig (▲), CD8 $^{+}$ depletion (▲) CD4 $^{+}$ depletion (○) or B cell depletion (□). (B) Mean tumor volume ($\text{mm}^3 \pm \text{SEM}$) after mice were injected with adjuvant (●) IGF-IR vaccine (○), or IGF-IR vaccine with isotype control Ig (▲) or IFN- γ depletion (○); ** $p<0.001$ for all panels.

with adjuvant induced similar tumor inhibition as vaccination with CD8⁺ ($p=0.376$) or B-cell depletion ($p=0.75$) or isotype control Ig (clg) treatment ($p=0.546$). However, depletion of CD4⁺ T-cells abrogated the anti-tumor effect of IGF-IR vaccination and tumor growth was no different from the adjuvant only controls, $p=0.339$ (Fig. 9A).

As the predominant cytokine secreted by the IGF-IR specific Th cells was IFN- γ , we selectively depleted IFN- γ in vaccinated mice prior to tumor challenge to determine its contribution to the observed anti-tumor activity. The average tumor volume in IFN- γ neutralized mice was significantly larger than untreated vaccinated mice ($p<0.0001$), or clg treated vaccinated mice ($p<0.0001$) (Fig. 9B). Indeed, tumor size in the vaccinated IFN- γ depleted animals was equivalent to adjuvant only controls ($p=0.207$).

Tumor proliferation was significantly decreased in the IGF-IR immunized animals compared to the adjuvant controls, $p<0.001$ (Fig. 10A and B). However, after IFN- γ depletion, the percentage of proliferating tumor cells in vaccinated mice was not significantly different from the control ($p=0.108$) (Fig. 10A), and was greater than that observed in tumors from vaccinated ($p<0.001$) and clg treated vaccinated mice ($p=0.008$) (Fig. 10A; representative fields Fig. 10B (I-IV)). In addition, apoptosis was significantly increased in tumors from both IGF-IR vaccinated and clg treated vaccinated mice compared to adjuvant only and IFN- γ depleted vaccinated mice ($p=0.002$, $p=0.01$, respectively) (Fig. 10C and D). There was no difference in apoptosis in IFN- γ depleted vaccinated mice and adjuvant control tumors ($p=0.575$) (Fig. 10C and D).

IFN- γ receptors are expressed on human breast cancer cells^{18,19} and we similarly demonstrate that IFN- γ -R1 is expressed on a syngeneic murine tumor cell line (Fig. 11A). *in vitro* IFN- γ treatment of human breast cancer cells has been shown to restore STAT1 signaling,²⁰ as it did in tumor cells (Fig. 11B). Figure 11B also demonstrates IFN- γ treatment of tumor cells inhibits signaling through IGF-IR without significantly altering receptor protein levels. As enhanced IGF-IR signaling has been shown to be associated with a loss of PTEN protein expression in breast cancer, conferring a growth advantage to PTEN negative cells,²¹ we assessed PTEN restoration with IFN- γ treatment. The level of PTEN protein was increased after IFN- γ exposure (Fig. 11B). As PTEN negatively regulates the PI3K/AKT pathway,²² we evaluated phospho-AKT expression after IFN- γ treatment, and demonstrated a marked decrease in activity (Fig. 11B).

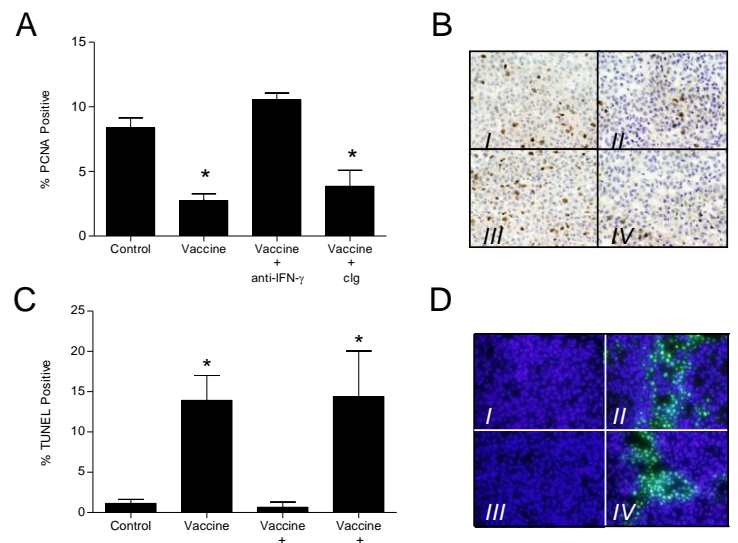


Figure 10. IFN- γ modulates tumor cell growth and survival. (A) Percent PCNA positive cells \pm SEM, in 21 day tumors, were counted from 10 high-powered fields (HPF) from 6 mice; * $p<0.01$. (B) Representative PCNA stain. (C) Percent TUNEL positive cells \pm SEM, in 21 day tumors, were counted from 10 high-powered fields (HPF) from 6 mice; * $p<0.01$. (B) Representative TUNEL stain; I: control; II: IGF-IR vaccine; III: vaccine + anti-IFN- γ ; IV: vaccine + clg.

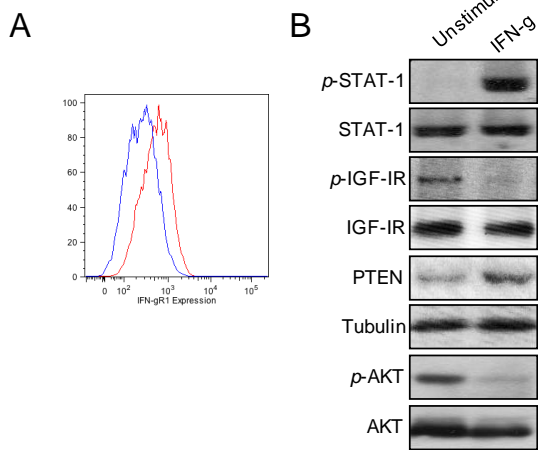


Figure 11. IGF-IR signaling is modulated by IFN-g. (A) Tumor cells were analyzed by flow cytometry; IgG isotype control (blue line), IFN-gR1 (red line). (B) Western blot of signaling proteins and tubulin,

protein expression in breast cancer, conferring a growth advantage to PTEN negative cells,²¹ we assessed PTEN restoration with IFN- γ treatment. The level of PTEN protein was increased after IFN- γ exposure (Fig. 11B). As PTEN negatively regulates the PI3K/AKT pathway,²² we evaluated phospho-AKT expression after IFN- γ treatment, and demonstrated a marked decrease in activity (Fig. 11B).

We questioned whether SOCS family members were operative in modulating IGF-IR signaling as SOCS proteins have been shown to attenuate signaling through insulin receptor, which is highly homologous.²³ Compared to SOCS2 and 3, SOCS1 expression in tumor cells was strongly induced with IFN- γ treatment (Fig. 12A). To determine whether SOCS1 was regulating IGF-IR phosphorylation in the presence of IFN- γ , we silenced its expression. Untreated MMC cells demonstrate high levels of IGF-IR phosphorylation which was significantly inhibited ($p=0.019$) with IFN- γ treatment in siRNA control cells (csirNA) (Fig. 12B I, III). Reduction of SOCS1 levels via siRNA, in the

presence of IFN- γ , resulted in 67% restoration of IGF-IR signaling, compared to IFN- γ csiRNA treated cells ($p=0.007$) (Fig. 12B *I, III*). IFN- γ inhibited proliferation of tumor cells treated with csiRNA compared to untreated cells ($p<0.0001$) (Fig. 12C,D). Decrease in SOCS1 expression, in the presence of IFN- γ did not significantly restore tumor proliferation to the level of the untreated control ($p<0.001$) but it did increase cell proliferation by 26% compared to csiRNA ($p<0.0001$) (Fig. 12C; representative fields Fig. 12D *I-III*).

Investigators have hypothesized that SOCS1 may directly interact with insulin receptor to inhibit activation of its downstream effectors²⁴ and we questioned whether SOCS1 may be directly binding to IGF-IR in our model. Figure 13 *I* demonstrates significant co-precipitation of SOCS1 with IGF-IR from IFN- γ -treated tumor cells compared to controls ($p=0.007$, Fig. 13 *I*).

Since overexpression of AKT induces Tamoxifen resistance, while inhibition restores Tamoxifen sensitivity,²⁵ we questioned whether our IGF-IR-specific vaccine would render previously Tamoxifen-resistant tumors now sensitive. Vaccination demonstrated an inhibition of tumor growth by 85% compared to adjuvant only control animals ($p<0.001$) (Fig. 14). Tumor growth in mice injected with adjuvant and treated with Tamoxifen was no different than that observed in untreated mice. However, treatment with Tamoxifen in vaccinated tumor-bearing mice resulted in a further 38% reduction in growth compared to vaccinated, untreated animals ($p=0.02$).

Aim 2.c. To determine whether IGF-IR vaccination induces diabetes or other toxicities in immunized mice.

Serum chemistries, complete blood count and pathology was performed on mice one week (acute toxicity) and 3 months (chronic toxicity) after the last vaccine.

All serum chemistry and complete blood count values for all groups were in the limits of the established ranges,²⁶⁻²⁹ except phosphorus, osmolality, chloride and platelet count (Tables 2-5, appendix). All groups of mice had a phosphorus value above the reference range (4.6-10.8 mg/dl) and osmolality values below the reference range (321-330). All groups except the IGF-IR vaccine group in the chronic toxicity cohort had a platelet count below the reference range (814-1656 K/uL). All groups in the chronic toxicity cohort had a chloride value below the reference range (110-204 meq/l). There was no significant difference in the values between any groups.

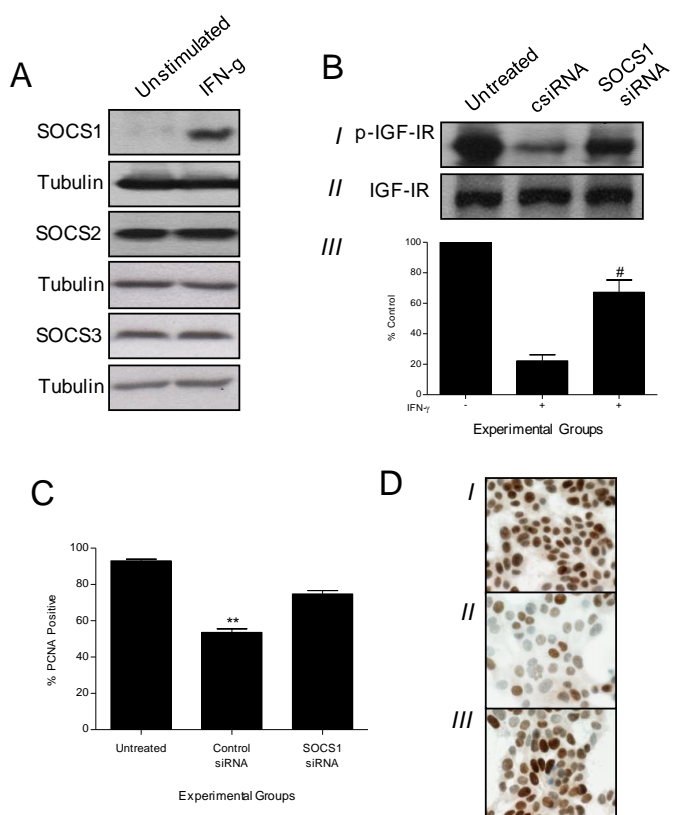


Figure 12. IFN- γ -induced SOCS1 mediates IGF-IR activity. (A) Western blot of SOCS family proteins, unstimulated and after IFN- γ treatment. (B) Representative Western blot of untreated and IFN- γ + control (c) siRNA and SOCS1 siRNA transfected MMC for phospho- (*I*) and total IGF-IR (*II*). Percent control of untreated cells \pm SEM as measured by densitometry for csiRNA and SOCS1 siRNA (*III*); * $p<0.01$ compared to csiRNA + IFN- γ treated cells ($n=3$ independent experiments). (C) Percent PCNA positive cells \pm SEM were counted from 10 HPF from 3 independent experiments for untreated and IFN- γ treated csiRNA and SOCS1 siRNA transfected tumor cells, ** $p<0.001$. (D) Representative PCNA stain; *I*: untreated; *II*: csiRNA + IFN- γ ; *III*: SOCS1 siRNA + IFN- γ .

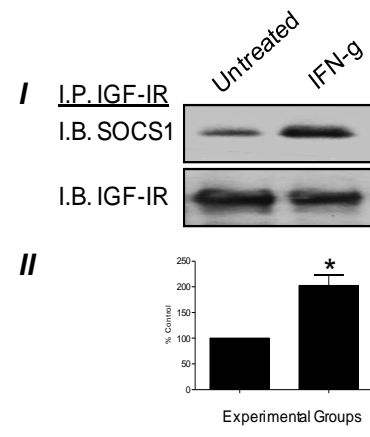


Figure 13. IFN- γ potentiates the association between SOCS1 and IGF-IR. Representative Western blot of co-immunoprecipitation of SOCS1 and IGF-IR from tumor cell lysate (*I*); I.P.: immunoprecipitation, I.B.: immunoblot. Densitometry is represented as percent control of untreated cells \pm SEM from three independent experiments (*II*); * $p<0.01$.

There were no treatment related lesions, which could be considered consistent with a toxic response that distinguished one group from another (Tables 6-11, appendix). The pancreas, thymus, ovary/uterus, heart, adrenal gland, skeletal muscle, brain and salivary gland contained no significant lesions in any of the groups in the acute toxicity cohort. The above mentioned organs were also without significant lesions in the chronic toxicity cohort except the adrenal gland, as some animals in all groups demonstrated mild lipofuscinoisis and X-zone vacuolation which is considered an incidental age-related lesion. Spleen and bone marrow were well populated with lymphoid cells in all animals and differences varied only slightly and were typically indistinguishable. Draining lymph nodes in the CFA and IGF-IR vaccinated groups contained lymphoid infiltrates consistent with ongoing immune stimulation. Liver, in most mice, had extramedullary hematopoiesis and mild random microgranuloma. In the lung in some of the vaccinated animals, there were perivascular lymphoid aggregates, consistent with an ongoing immune response. These findings were mild and of no clinical consequence. There was minimal to mild renal tubule hypertrophy and hyperplasia in some of the mice. However, since this result was observed in the untreated mice, we concluded it was not a result of vaccination with IGF-IR. Of note, all 30 animals were alive and appeared healthy following the final vaccination.

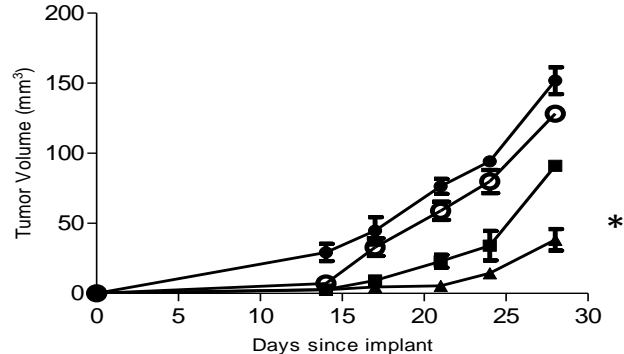


Figure 14. IGF-IR-specific vaccine sensitizes tumors to Tamoxifen therapy. Mean tumor volume (\pm SEM) of mice injected with adjuvant (●), IGF-IR vaccine (■), or treated with Tamoxifen after injection of adjuvant (○) or IGF-IR vaccine (▲). * $p<0.001$; n=5 mice / group.

Training Program.

My mentor and I have had intensive one-on-one meetings once every two weeks to evaluate the status of the project. I have attended our general laboratory research meetings every week where I have presented data eight different times. In addition, I have attended two different focused small group lab meetings on vaccine design and development every week where I have presented data as well as given introductory lectures on new concepts within my scope of work that was unknown to the group.

I have attended and presented my data at the annual American Association of Cancer Research meeting and the Era of Hope Meeting. I presented data as an invited speaker for the Mexican Northwest Oncology Group as well as a guest lecturer for the University of Washington's Department of Pharmaceutics.

I have participated in many seminars and short courses offered by the University of Washington's Institute for Translational Health Sciences on career development and clinical education. I have also witnessed the consent process involved in enrolling a patient on a clinical trial.

I have worked closely with my mentor on submitting a pilot grant and the preparation of three manuscripts.

KEY RESEARCH ACCOMPLISHMENTS

- There was no difference in the magnitude and incidence of the Th1 immune response to any individual IGF-IR peptide between cancer and volunteers.
- IGF-IR Th1 immunity is associated with increased adiposity.
- CTD peptides induce a significantly greater inflammatory Th1 response with significantly less Th2 immunity in most patients tested.
- Vaccination with the IGF-IR-CTD peptide pool stimulates a Th1 immune response and inhibits tumor growth in the TgC3(I)-Tag mouse model of TNBC.
- Th1 cells, elicited by IGF-IR vaccination, inhibit the growth of breast cancer via IFN- γ secretion.
- IFN- γ regulates tumor cell growth and survival via SOCS1-dependent inhibition of IGF-IR signaling.
- IGF-IR-specific vaccine sensitizes tumors to Tamoxifen therapy.
- No toxicities were observed following vaccination with IGF-IR peptides.

REPORTABLE OUTCOMES

Abstracts:

Vaccination with peptides in IGF-IR that induce robust Th1 immunity with limited immunosuppression significantly inhibit tumor growth in a model of triple-negative breast cancer. Department of Defense Breast Cancer Research Program Era of Hope Meeting, 2011.

Vaccination targeting IGF-IR sensitizes tumors to tamoxifen therapy in an anti-estrogen resistant mouse model. American Association of Cancer Research Annual Meeting, 2012.

Publication:

Cecil DL, Park K, Gad E, Childs JS, Higgins DM, Plymate SR, Disis ML. T-helper 1 immunity, specific for the breast cancer antigen insulin-like growth factor-I receptor (IGF-IR), is associated with increased adiposity. *Breast Cancer Res Treat.* 2013; 139(3):657-665.

CONCLUSION

TNBC is considered more clinically aggressive than other breast cancer phenotypes: patients who develop metastatic TNBC have a shorter survival than patients with metastatic breast cancer of other subtypes and the majority of deaths occur within the first 5 years after therapy is completed.³⁰ But, if a TNBC patient can achieve a complete remission with standard therapy, their chance at survival is similar to other better prognosis breast cancer subtypes.³¹ Data generated in this fellowship has paved the way for a more effective vaccine targeting this aggressive breast cancer phenotype.

The ability to more effectively treat cancer after immunization, or other forms of Type 1 cytokine inducing immune therapy, may contribute to the survival benefit observed after immunization in clinical trials of cancer vaccines.³²⁻³⁴ Our data would suggest that vaccine-induced oncogenic shock plays a role in sensitizing tumors to enhanced cell death with subsequent treatment. Planned future studies will determine if IGF-IR vaccine-induced sensitization to therapy applies to other common chemotherapies, such as taxol, in TNBC. A clinical trial will be planned that combines the IGF-IR vaccine with standard therapy.

An alternative line of study generated from this fellowship stems from the observation that IGF-IR is a potential obesity-associated antigen. Obesity, especially obesity which is linked with insulin resistance, diabetes and hypertension (metabolic syndrome) is a precursor physiology for the development of breast cancer. Obesity is a risk factor for TNBC. One analysis of nearly 200 women observed 58% of patients with TNBC had evidence of metabolic syndrome.³⁵ Chronic inflammation, with marked Type 1 inflammatory infiltrates, established in obese breast tissue lays the foundation for eventual malignant transformation. Th2 cells have been shown to halt and even reverse the abnormal Type 1 inflammation of obesity in mouse models. Mice fed with a high fat diet which resulted in adipose inflammation were treated with adoptive transfer of Th2 secreting IL-4 and IL-13.³⁶ The infused Th2 reversed the weight gain and resolved insulin resistance in treated mice compared to untreated controls. We hypothesize that a vaccine targeting immunogenic proteins, up-regulated in adipocytes at the start of inflammatory obesity, designed to elicit Th2 cells could directly impact the tissues where Type 1 inflammation was occurring. Data generated from this fellowship has identified potential Th2-inducing epitopes in IGF-IR. Such a vaccine could be given to overweight women to prevent the development of breast cancer.

REFERENCES

1. Sharma, S.V., et al. A common signaling cascade may underlie "addiction" to the Src, BCR-ABL, and EGF receptor oncogenes. *Cancer Cell.* **10**, 425-435. (2006).
2. Cao, L., et al. Addiction to elevated insulin-like growth factor I receptor and initial modulation of the AKT pathway define the responsiveness of rhabdomyosarcoma to the targeting antibody. *Cancer Res.* **68**, 8039-8048. (2008).
3. Weinstein, I.B. & Joe, A. Oncogene addiction. *Cancer research* **68**, 3077-3080; discussion 3080 (2008).
4. McDermott, U., Pusapati, R.V., Christensen, J.G., Gray, N.S. & Settleman, J. Acquired resistance of non-small cell lung cancer cells to MET kinase inhibition is mediated by a switch to epidermal growth factor receptor dependency. *Cancer research* **70**, 1625-1634 (2010).
5. Wheeler, C.J., Das, A., Liu, G., Yu, J.S. & Black, K.L. Clinical responsiveness of glioblastoma multiforme to chemotherapy after vaccination. *Clinical cancer research : an official journal of the American Association for Cancer Research* **10**, 5316-5326 (2004).
6. Salazar, L.G., et al. Immunization of cancer patients with HER-2/neu-derived peptides demonstrating high-affinity binding to multiple class II alleles. *Clinical cancer research : an official journal of the American Association for Cancer Research* **9**, 5559-5565 (2003).
7. Park, K.H., et al. Insulin-like growth factor-binding protein-2 is a target for the immunomodulation of breast cancer. *Cancer research* **68**, 8400-8409 (2008).
8. Vignali, D.A., Collison, L.W. & Workman, C.J. How regulatory T cells work. *Nature reviews. Immunology* **8**, 523-532 (2008).
9. Vence, L., et al. Circulating tumor antigen-specific regulatory T cells in patients with metastatic melanoma. *Proceedings of the National Academy of Sciences of the United States of America* **104**, 20884-20889 (2007).
10. Guerkov, R.E., et al. Detection of low-frequency antigen-specific IL-10-producing CD4(+) T cells via ELISPOT in PBMC: cognate vs. nonspecific production of the cytokine. *Journal of immunological methods* **279**, 111-121 (2003).
11. Ruffatti, A., et al. Autoantibodies of systemic rheumatic diseases in the healthy elderly. *Gerontology* **36**, 104-111 (1990).
12. Attanasio, R., et al. Age-related autoantibody production in a nonhuman primate model. *Clinical and experimental immunology* **123**, 361-365 (2001).
13. Tachikawa, S., et al. Appearance of B220low autoantibody-producing B-1 cells at neonatal and older stages in mice. *Clinical and experimental immunology* **153**, 448-455 (2008).
14. Viardot, A., et al. Obesity is associated with activated and insulin resistant immune cells. *Diabetes/metabolism research and reviews* **28**, 447-454 (2012).
15. Bäck, A.H. Changes in insulin and IGF-I receptor expression during differentiation of human preadipocytes. *Growth Horm IGF Res.* **19**, 101-111 (2009).
16. Holzer, R.G., et al. Development and characterization of a progressive series of mammary adenocarcinoma cell lines derived from the C3(1)/SV40 Large T-antigen transgenic mouse model. *Breast cancer research and treatment* **77**, 65-76 (2003).
17. Plymate, S.R., et al. An antibody targeting the type I insulin-like growth factor receptor enhances the castration-induced response in androgen-dependent prostate cancer. *Clin Cancer Res.* **13**, 6429-6439. (2007).
18. Khalkhali-Ellis, Z., et al. IFN-gamma regulation of vacuolar pH, cathepsin D processing and autophagy in mammary epithelial cells. *J Cell Biochem.* **105**, 208-218. (2008).
19. Garcia-Tunon, I., et al. Influence of IFN-gamma and its receptors in human breast cancer. *BMC Cancer.* **7**, 158. (2007).
20. Gooch, J.L., Herrera, R.E. & Yee, D. The role of p21 in interferon gamma-mediated growth inhibition of human breast cancer cells. *Cell Growth Differ.* **11**, 335-342. (2000).
21. Miller, T.W., et al. Loss of Phosphatase and Tensin homologue deleted on chromosome 10 engages ErbB3 and insulin-like growth factor-I receptor signaling to promote antiestrogen resistance in breast cancer. *Cancer Res.* **69**, 4192-4201. Epub 2009 May 4112. (2009).

22. Jiang, B.H. & Liu, L.Z. PI3K/PTEN signaling in angiogenesis and tumorigenesis. *Adv Cancer Res.* **102**, 19-65. (2009).
23. McGillicuddy, F.C., et al. Interferon gamma attenuates insulin signaling, lipid storage, and differentiation in human adipocytes via activation of the JAK/STAT pathway. *J Biol Chem.* **284**, 31936-31944. Epub 32009 Sep 31923. (2009).
24. Mooney, R.A., et al. Suppressors of cytokine signaling-1 and -6 associate with and inhibit the insulin receptor. A potential mechanism for cytokine-mediated insulin resistance. *J Biol Chem.* **276**, 25889-25893. Epub 22001 May 25887. (2001).
25. Clark, A.S., West, K., Streicher, S. & Dennis, P.A. Constitutive and inducible Akt activity promotes resistance to chemotherapy, trastuzumab, or tamoxifen in breast cancer cells. *Molecular cancer therapeutics* **1**, 707-717 (2002).
26. <http://phenome.jax.org>. (2013).
27. Mazzaccara, C., et al. Age-Related Reference Intervals of the Main Biochemical and Hematological Parameters in C57BL/6J, 129SV/EV and C3H/HeJ Mouse Strains. *PLoS one* **3**, e3772 (2008).
28. <http://hilltoplabs.com/public/blood.html>. (2013).
29. Zaias, J., Mineau, M., Cray, C., Yoon, D. & Altman, N.H. Reference values for serum proteins of common laboratory rodent strains. *Journal of the American Association for Laboratory Animal Science : JAALAS* **48**, 387-390 (2009).
30. Dent, R., et al. Triple-negative breast cancer: clinical features and patterns of recurrence. *Clinical cancer research : an official journal of the American Association for Cancer Research* **13**, 4429-4434 (2007).
31. Carey, L.A., et al. The triple negative paradox: primary tumor chemosensitivity of breast cancer subtypes. *Clinical cancer research : an official journal of the American Association for Cancer Research* **13**, 2329-2334 (2007).
32. Disis, M.L., et al. Concurrent trastuzumab and HER2/neu-specific vaccination in patients with metastatic breast cancer. *Journal of clinical oncology : official journal of the American Society of Clinical Oncology* **27**, 4685-4692 (2009).
33. Kantoff, P.W., et al. Sipuleucel-T immunotherapy for castration-resistant prostate cancer. *The New England journal of medicine* **363**, 411-422 (2010).
34. Kantoff, P.W., et al. Overall survival analysis of a phase II randomized controlled trial of a Poxviral-based PSA-targeted immunotherapy in metastatic castration-resistant prostate cancer. *Journal of clinical oncology : official journal of the American Society of Clinical Oncology* **28**, 1099-1105 (2010).
35. Maiti, B., Kundranda, M.N., Spiro, T.P. & Daw, H.A. The association of metabolic syndrome with triple-negative breast cancer. *Breast cancer research and treatment* **121**, 479-483 (2010).
36. Winer, S., et al. Normalization of obesity-associated insulin resistance through immunotherapy. *Nature medicine* **15**, 921-929 (2009).

APPENDICES

Table 2: Summary of acute serum chemistries for all groups (median and range).

Parameter (units)	CFA/IFA	range	IGF-IR peptides	range	Control (untreated)	range
Glucose (mg/dl)	180	55-243	75	52-173	78	59-103
BUN (mg/dl)	28	26-28	29	24-31	26	20-30
Creatinine (mg/dl)	0.2	0.2-0.3	0.2	0.2-0.2	0.2	0.2-0.2
Sodium (meq/dl)	150	147-153	151	149-151	152	151-154
Potassium (meq/dl)	8.1	7.4-9.1	8.6	8.3-9.4	8	7.7-9.9
Sodium/Potassium Ratio	19	17-20	18	16-18	19	16-20
Chloride (meq/dl)	108	104-109	106	106-108	106	105-112
Carbon Dioxide (meq/dl)	24	15-27	23	21-27	26	16-27
Anion Gap	26	25-34	30	37-31	28	27-36
Calcium (mg/dl)	9.6	9.3-10	9.8	9.6-10.2	9.8	9.7-10.8
Phosphorus (mg/dl)	17.3	15.4-19.2	16.8	14.9-17.4	15.9	14.4-17.1
Osmolality	314	311-315	312	308-313	310	307-311
Protein (g/dl)	4.5	4.1-4.9	5.1	4.6-5.1	5.1	4.8-5.3
Albumin (g/dl)	2.9	2.7-3.1	3.2	2.8-3.2	3.3	3-3.3
Globulin (g/dl)	1.6	1.4-1.8	2	1.8-2.2	1.9	1.8-2
Albumin/Globulin Ratio	1.8	1.6-1.9	1.6	1.5-1.7	1.7	1.7-1.8
Bilirubin (mg/dl)	0.2	0.1-0.2	0.2	0.1-0.2	0.2	0.2-0.2
AlkPhos (U/L)	105	82-123	104	92-122	132	114-155
GGT (U/L)	0	0-1	0	0	1	0-1
ALT (U/L)	41	33-62	46	43-50	43	41-62
AST (U/L)	104	83-222	118	98-155	140	93-207
Cholesterol (mg/dl)	117	106-124	139	123-157	149	139-152

Table 3: Summary of acute CBC for all groups (median and range).

Parameter (units)	CFA/IFA	range	IGF-IR peptides	range	Control (untreated)	range
WBC (K/uL)	3.1	0.8-10.8	2.7	1.4-5.1	4.4	2.8-6.7
RBC (M/uL)	8.72	7.36-9.84	9.68	8.04-10.4	9.52	9.12-10.04
HGB (g/dL)	12	10.8-13.6	14.6	11.6-15.2	14	12.8-14.8
HCT (%)	44	42.4-49.6	48.8	40.4-51.2	46.4	43.2-48.4
MCV (fL)	50.8	49.4-52.5	50	49.8-50.5	48.5	47.4-49
MCH (pg)	13.9	13.5-15.2	14.3	13.5-15.1	14.4	13.6-14.8
MCHC (%)	27.4	26.4-30.7	29.1	26.8-29.9	29.7	29.7-30.8
Platelet Count (K/uL)	800	350-984	1148	1016-1258	716	352-864
Polys (%)	6	4-14	6	3-18	2	1-5
Lymph (%)	91	80-92	92	78-95	94	92-97
Monos (%)	3	1-4	2	1-4	1	1-4
Eos (%)	2	0-4	0	0-1	1	0-2
Baso (%)	0	0	0	0	0	0

Table 4: Summary of chronic serum chemistries for all groups (median and range).

Parameter (units)	CFA/IFA	range	IGF-IR peptides	range	Control (untreated)	range
Glucose (mg/dl)	151	42-214	122	69-233	153	51-195
BUN (mg/dl)	28	27-33	28	26-31	28	25-29
Creatinine (mg/dl)	0.2	0.2-0.3	0.3	0.2-0.3	0.3	0.2-0.3
Sodium (meq/dl)	152	149-153	152	149-153	150	149-155
Potassium (meq/dl)	8.1	7.7-9.6	9.3	7.7-10	8.6	8.5-9.9
Sodium/Potassium Ratio	19	18-20	16	15-19	18	15-19
Chloride (meq/dl)	108	106-110	108	105-109	106	105-108
Carbon Dioxide (meq/dl)	20	17-23	18	10-23	16	13-24
Anion Gap	34	29-34	34	32-43	34	29-43
Calcium (mg/dl)	9.8	9.1-9.8	10.3	9.6-11.1	9.5	9.3-10.2
Phosphorus (mg/dl)	19.6	18.2-20.1	21.2	20.8-22.4	16.7	15.7-19.8
Osmolality	316	311-321	315	315-318	313	310-319

Protein (g/dl)	4.7	4.7-5.5	4.9	4.6-5.4	5.2	4.7-5.4
Albumin (g/dl)	2.7	2.6-3.1	2.9	2.6-3.1	3	2.8-3.1
Globulin (g/dl)	2	1.7-2.4	2.2	2-2.4	2.1	1.9-2.3
Albumin/Globulin Ratio	1.4	1.3-1.5	1.3	1.2-1.5	1.5	1.3-1.5
Bilirubin (mg/dl)	0.1	0.1-0.2	0.1	0.1	0.1	0.1
AlkPhos (U/L)	82	78-98	102	94-114	105	94-116
GGT (U/L)	0	0	0	0	0	0
ALT (U/L)	51	29-51	50	36-54	58	371-65
AST (U/L)	98	81-137	109	90-278	121	87-243
Cholesterol (mg/dl)	111	96-153	122	117-142	129	109-139

Table.5: Summary of chronic CBC for all groups (median and range).

Parameter (units)	CFA/IFA	range	IGF-IR peptides	range	Control (untreated)	range
WBC (K/uL)	2.1	1.8-3.8	1.8	1.1-2.1	2.2	1.3-6.7
RBC (M/uL)	8.2	3.6-8.8	8.74	7.76-9.92	8.44	7.12-9.44
HGB (g/dL)	12.4	11.6-13.2	13.2	11.6-15.2	12.8	12.4-14.4
HCT (%)	42	38-43.6	42.4	38.8-51.3	42.4	41.2-46.8
MCV (fL)	48.7	47.7-50.4	48.6	48.2-52.1	49	47.7-49
MCH (pg)	14.5	14.2-15.2	14.9	14.5-15.4	15.1	14.8-15.1
MCHC (%)	30	28.8-30.7	30	29-31.6	30.7	30.2-31.6
Platelet Count (K/uL)	772	408-800	676	416-818	552	256-808
Polys (%)	5	2-6	5	2-9	3	2-15
Lymph (%)	94	93-97	94	90-97	97	84-97
Monos (%)	1	0-2	1	0-1	0	0-1
Eos (%)	0	0-2	0	0-1	0	0-1
Baso (%)	0	0	0	0	0	0

Table 6. Pathology of CFA vaccinated mice (acute).

Organ	Mouse 1	Mouse 2	Mouse 3	Mouse 4	Mouse 5
Bone Marrow	mild granulocytic hyperplasia	mild granulocytic hyperplasia	mild granulocytic hyperplasia	mild granulocytic hyperplasia	mild granulocytic hyperplasia
Muscle	NSL	NSL	NSL	NSL	NSL
Brain	NSL	NSL	NSL	NSL	NSL
Lung	NSL	NSL	Moderate coalescing histiocytic pneumonia with hemorrhage and acidophilic macrophages, some foamy macrophages, chronic.	NSL	NSL
Heart	NSL	NSL	minimal right ventricular dilation	NSL	NSL
Thymus	N/A	NSL	NSL	NSL	NSL
Liver	mild MF random MG and EMH	mild MF random MG and EMH	mild MF random MG and EMH	mild MF random MG and EMH, focal acute coagulative necrosis	mild MF random MG and EMH
Kidney	tubular hypertrophy/hyperplasia MF mild	tubular hypertrophy/hyperplasia MF mild	focal mild cortical cyst	tubular hypertrophy/hyperplasia MF mild	NSL
Pancreas	NSL	NSL	NSL	NSL	NSL
Spleen	NSL	NSL	NSL	moderate lymphocytic hyperplasia	moderate lymphocytic hyperplasia
Adrenal	NSL	NSL	NSL	NSL	NSL
Ovary	NSL	NSL	NSL	NSL	NSL
Uterus	NSL	NSL	NSL	NSL	NSL

Lymph node	Mild hyperplasia and moderate granulomatous perinodal cellulitis	mild hyperplasia	mild hyperplasia and granulomatous lymphadenitis with free lipid	NSL	Mild hyperplasia and moderate granulomatous perinodal cellulitis and steatosis, chronic.
Salivary glands	NSL	NSL	NSL	NSL	NSL
Comment	There is no evidence of any test-related lesions in any of the tissues examined	There is no evidence of any test-related lesions in any of the tissues examined	There is no evidence of any test-related lesions in any of the tissues examined	There is no evidence of any test-related lesions in any of the tissues examined	There is no evidence of any test-related lesions in any of the tissues examined

NSL: no significant lesion

MF: multifocal

MG: microgranuloma

EMH: extramedullary hematopoiesis

Table 7. Pathology of IGF-IR vaccinated mice (acute).

Organ	Mouse 11	Mouse 12	Mouse 13	Mouse 14	Mouse 15
Bone Marrow	mild granulocytic hyperplasia	mild granulocytic hyperplasia	mild granulocytic hyperplasia	mild granulocytic hyperplasia	mild granulocytic hyperplasia
Muscle	NSL	NSL	NSL	NSL	NSL
Brain	NSL	NSL	NSL	NSL	NSL
Lung	NSL	NSL	NSL	NSL	minimal multifocal histiocytic lesser neutrophilic perivascular and interstitial accumulations
Heart	mild focal acute myocardial hemorrhage	NSL	NSL	NSL	NSL
Thymus	NSL	NSL	NSL	NSL	NSL
Liver	mild MF random MG and EMH	NSL	mild MF random MG and EMH	mild MF random MG and EMH	mild MF random MG and EMH
Kidney	minimal tubular hyperplasia	NSL	NSL	NSL	mild multifocal tubular hyperplasia
Pancreas	NSL	NSL	NSL	NSL	NSL
Spleen	mild lymphocytic hyperplasia	mild lymphocytic hyperplasia	moderate lymphocytic hyperplasia	moderate lymphocytic hyperplasia	moderate lymphocytic hyperplasia
Adrenal	NSL	NSL	NSL	NSL	NSL
Ovary	NSL	NSL	NSL	NSL	NSL
Uterus	NSL	NSL	NSL	NSL	NSL
Lymph node	marked perinodal (?) granulomatous and fibrosing cellulitis and steatitis with multifocal microabcesses	minimal sinusoidal histiocytosis with lipid	mild perinodal granulomatous and fibrosing cellulitis and steatitis with multifocal microabcesses	minimal perinodal granulomatous and fibrosing cellulitis and steatitis with multifocal microabcesses	moderate hyperplasia and granulomatous lymphadenitis with free lipid
Salivary glands	draining hemorrhage, mild	NSL	NSL	NSL	NSL
Comment	There is no evidence of any test-related lesions in any of the tissues examined	There is no evidence of any test-related lesions in any of the tissues examined	There is no evidence of any test-related lesions in any of the tissues examined	There is no evidence of any test-related lesions in any of the tissues examined	There is no evidence of any test-related lesions in any of the tissues examined

NSL: no significant lesion

MF: multifocal

MG: microgranuloma

EMH: extramedullary hematopoiesis

Table 8. Pathology of untreated mice (acute).

Organ	Mouse 21	Mouse 22	Mouse 23	Mouse 24	Mouse 25
Bone Marrow	mild granulocytic hyperplasia				
Muscle	NSL	NSL	NSL	NSL	NSL
Brain	NSL	NSL	NSL	NSL	NSL
Lung	NSL	NSL	NSL	NSL	NSL
Heart	NSL	NSL	NSL	NSL	NSL
Thymus	NSL	NSL	NSL	NSL	NSL
Liver	mild MF random MG and EMH	NSL			
Kidney	mild multifocal tubular hyperplasia	mild multifocal tubular hyperplasia	NSL	NSL	NSL
Pancreas	NSL	NSL	NSL	NSL	NSL
Spleen	mild lymphocytic hyperplasia	mild lymphocytic hyperplasia	moderate lymphocytic hyperplasia	moderate lymphocytic hyperplasia	moderate lymphocytic hyperplasia
Adrenal	NSL	NSL	NSL	NSL	NSL
Ovary	NSL	NSL	NSL	NSL	NSL
Uterus	NSL	NSL	NSL	NSL	NSL
Lymph node	moderate hyperplasia and granulomatous lymphadenitis with free lipid	mild chronic draining hemorrhage	NSL	NSL	NSL
Salivary glands	NSL	NSL	NSL	NSL	NSL
Comment	There is no evidence of any test-related lesions in any of the tissues examined	There is no evidence of any test-related lesions in any of the tissues examined	There is no evidence of any test-related lesions in any of the tissues examined	There is no evidence of any test-related lesions in any of the tissues examined	There is no evidence of any test-related lesions in any of the tissues examined

NSL: no significant lesion

MF: multifocal

MG: microgranuloma

EMH: extramedullary hematopoiesis

Table 9. Pathology of CFA vaccinated mice (chronic).

Organ	Mouse 6	Mouse 7	Mouse 8	Mouse 9	Mouse 10
Bone Marrow	mild granulocytic hyperplasia	mild granulocytic hyperplasia	mild granulocytic hyperplasia	mild granulocytic hyperplasia	mild granulocytic hyperplasia
Muscle	NSL	NSL	NSL	NSL	NSL
Brain	NSL	NSL	NSL	NSL	NSL
Lung	NSL	NSL	MF mild PV lymphoid aggregates	NSL	NSL
Heart	NSL	NSL	NSL	NSL	NSL
Liver	minimal random MG and EMH	minimal random MG and EMH	mild random MG and EMH	mild random MG and EMH	minimal random MG and EMH
Kidney	NSL	mild focal tubular hypertrophy	NSL	NSL	mild MF tubular hyperplasia
Pancreas	NSL	NSL	NSL	NSL	
Spleen	mild lymphocytic hyperplasia	mild lymphocytic hyperplasia	Moderate lymphocytic hyperplasia and extramedullary hematopoiesis	mild lymphocytic hyperplasia	mild lymphocytic hyperplasia
Adrenal	Mild lipofuscinoisis and X-zone vacuolation	NSL	Mild lipofuscinoisis and X-zone vacuolation	NSL	Mild lipofuscinoisis and X-zone vacuolation
Thymus	NSL	NSL	NSL	NSL	NSL
Ovary	NSL	NSL	NSL	NSL	NSL

Uterus	NSL	NSL	NSL	NSL	NSL
Lymph node	NSL	mild focally extensive perinodal granulomatous and necrotizing steatitis	moderate diffuse granulomatous adenitis with free lipid	moderate diffuse granulomatous adenitis with free lipid	moderate diffuse granulomatous adenitis with free lipid and perinodal
Salivary gland	NSL	NSL	NSL	NSL	NSL
Comment	There is no evidence of any test-related lesions in any of the tissues examined	There is no evidence of any test-related lesions in any of the tissues examined	There is no evidence of any test-related lesions in any of the tissues examined	There is no evidence of any test-related lesions in any of the tissues examined	There is no evidence of any test-related lesions in any of the tissues examined

NSL: no significant lesion

MF: multifocal

MG: microgranuloma

EMH: extramedullary hematopoiesis

PV: perivascular

Table 10. Pathology of IGF-IR vaccinated mice (chronic).

Organ	Mouse 16	Mouse 17	Mouse 18	Mouse 19	Mouse 20
Bone Marrow	mild granulocytic hyperplasia	mild granulocytic hyperplasia	mild hyperplasia	mild hyperplasia	mild hyperplasia
Muscle	NSL	NSL	NSL	NSL	NSL
Brain	NSL	NSL	NSL	NSL	NSL
Lung	minimal mf pv lymphoid accumulations		minimal mf pv lymphoid accumulations	NSL	NSL
Heart	NSL	NSL	NSL	NSL	NSL
Liver	mild random MG and EMH	minimal random MG and EMH	minimal random MG and EMH	minimal random MG and EMH	minimal random MG and EMH
Kidney	NSL	NSL	NSL	NSL	NSL
Pancreas	NSL	NSL	NSL	NSL	NSL
Spleen	mild lymphocytic hyperplasia	mild lymphocytic hyperplasia and red pulp hemosiderin accumulation	mild lymphocytic hyperplasia and red pulp hemosiderin accumulation	mild lymphocytic hyperplasia	mild lymphocytic hyperplasia
Adrenal	NSL	incidental, age associated lesion	Mild lipofuscinoisis and X-zone vacuolation	Mild lipofuscinoisis and X-zone vacuolation	NSL
Thymus	NSL	NSL	NSL	NSL	NSL
Ovary	NSL	NSL	NSL	NSL	NSL
Uterus	NSL	NSL	NSL	NSL	NSL
Lymph node	mild granulomatous adenitis	moderate granulomatous adenitis	moderate granulomatous adenitis	N/A	moderate granulomatous adenitis
Salivary gland	NSL	NSL	NSL	NSL	NSL
Comment	There is no evidence of any test-related lesions in any of the tissues examined	There is no evidence of any test-related lesions in any of the tissues examined	There is no evidence of any test-related lesions in any of the tissues examined	There is no evidence of any test-related lesions in any of the tissues examined	There is no evidence of any test-related lesions in any of the tissues examined

NSL: no significant lesion

MF: multifocal

MG: microgranuloma

EMH: extramedullary hematopoiesis

PV: perivascular

Table 11. Pathology of untreated mice (chronic).

Organ	Mouse 26	Mouse 27	Mouse 28	Mouse 29	Mouse 30
Bone Marrow	mild hyperplasia				
Muscle	NSL	NSL	NSL	NSL	NSL
Brain	NSL	NSL	NSL	NSL	NSL
Lung	NSL	NSL	NSL	NSL	NSL
Heart	NSL	NSL	NSL	NSL	NSL
Liver	minimal random MG and EMH	moderate random MG and EMH	moderate random MG and EMH	minimal random MG and EMH	mild hyperplasia
Kidney	NSL	NSL	minimal focal tubular hyperplasia	mild multifocal tubular hyperplasia	mild multifocal tubular hyperplasia
Pancreas	NSL	NSL	NSL	NSL	NSL
Spleen	mild red pulp hemosiderin	NSL	NSL	mild lymphocytic hyperplasia	NSL
Adrenal	Mild lipofuscinoisis and X-zone vacuolation	mild subcapsular spindle cell hyperplasia	Mild lipofuscinoisis and X-zone vacuolation	NSL	NSL
Thymus	NSL	NSL	NSL	NSL	NSL
Ovary	NSL	NSL	NSL	NSL	NSL
Uterus	NSL	NSL	NSL	NSL	NSL
Lymph node	NSL	NSL	NSL	NSL	NSL
Salivary gland	NSL	NSL	NSL	NSL	NSL
Comment	There is no evidence of any test-related lesions in any of the tissues examined	There is no evidence of any test-related lesions in any of the tissues examined	There is no evidence of any test-related lesions in any of the tissues examined	There is no evidence of any test-related lesions in any of the tissues examined	There is no evidence of any test-related lesions in any of the tissues examined

NSL: no significant lesion

MF: multifocal

MG: microgranuloma

EMH: extramedullary hematopoiesis

Abstracts:

The insulin-like growth factor (IGF) pathway plays an important role in breast cancer growth and metastasis. The IGF-I receptor (IGF-IR) is overexpressed in almost 50% of triple negative breast cancers (TNBC), defined as estrogen (ER) and progesterone (PR) receptor and HER-2/neu receptor (HER2) negative. Thus, therapeutically targeting tumor cells which have upregulated IGF-IR may be a promising approach to treat TNBC. We have determined that IGF-IR is immunogenic in breast cancer and is a potential target for active immunization. Our aim is to develop vaccines that will elicit Th1 immunity to IGF-IR. Antigen specific Th1 can modulate the tumor microenvironment to enhance cross priming, supporting the proliferation of cytotoxic T cells which are capable of eradicating breast cancer cells. Since it has been demonstrated that natural immunogenic human epitopes can be predicted by high binding affinity across multiple class II alleles, we used a combined scoring system from five algorithms for predicting class II binding to determine Th epitopes of IGF-IR and identified 20 potentially immunogenic peptides. We observed that 95% of the peptides predicted induced a Th1 immune response as measured by IFN-gamma ELISPOT in human PBMC. However, IGF-IR is a "self" tumor antigen, thus, Th epitopes could potentially elicit either an inflammatory Th1 or immunosuppressive Th2 response, characterized by secretion of cytokines such as IL-10. To determine the propensity of a peptide to induce a Th1 or Th2 response, we created a ratio of IFN-gamma to IL-10 that analyzed both the magnitude and frequency of ELISPOT responses for each peptide. We demonstrated that

60% of the peptides show a preference to secrete IFN-gamma over IL-10 and those peptides were located primarily in the C-terminal intracellular portion of the protein. Thus, this area would likely be ideal for a multi-epitope vaccine. Vaccination with peptides p1166-1181, p1212-1227, p1301-1316, 1307-1322 and p1311-1326 in C3T(ag) mice demonstrated a robust Th1 response and concomitant inhibition of tumor growth by 85% compared to adjuvant only control animals. These data suggest that more effective peptide-based vaccines can be designed when both Th1 epitopes and immunosuppressive epitopes are screened simultaneously and epitopes that are most likely to induce robust Th1 responses in the majority of individuals can be identified and included as vaccine components.

Tamoxifen is a standard treatment for estrogen receptor (ER)-positive breast cancer patients. However, acquired or de novo resistance to therapy is a major clinical problem. In hormone-resistant tumors, there is increased activation of insulin-like growth factor-1 receptor (IGF-IR) and subsequent downstream signaling molecules, such as AKT. We have determined that IGF-IR is immunogenic in breast cancer and is a potential target for active immunization. It has been demonstrated that natural immunogenic human epitopes can be predicted by high binding affinity across multiple class II alleles, thus, we used a combined scoring system from five algorithms for predicting class II binding to determine Th epitopes of IGF-IR. Of the 20 potentially immunogenic peptides identified, five peptides (p1166-1181, p1212-1227, p1301-1316, 1307-1322 and p1311-1326) in the C-terminal domain were determined to elicit a predominantly inflammatory Th1 response compared to an immunosuppressive Th2 response in human PBMC. Overexpression of AKT induces tamoxifen resistance, while inhibition restores tamoxifen sensitivity. The tumor suppressor, PTEN, actively inhibits AKT. Data we have generated demonstrated that vaccination restored PTEN activity in tumor cells. We questioned if modulation of PTEN could render tumors in the anti-estrogen-resistant MMTV-neu mouse model sensitive to tamoxifen therapy. Vaccination demonstrated a robust Th1 response ($p<0.001$) and concomitant inhibition of tumor growth by 85% compared to adjuvant only control animals ($p<0.001$). Treatment with tamoxifen in vaccinated tumor-bearing mice resulted in a further 38% reduction in growth ($p=0.02$). Thus, active immunization targeting IGF-IR may induce both immunologic and biologic effects resulting in the sensitization of the tumor to tamoxifen therapy.

T-helper I immunity, specific for the breast cancer antigen insulin-like growth factor-I receptor (IGF-IR), is associated with increased adiposity

Denise L. Cecil · Kyong Hwa Park ·
Ekram Gad · Jennifer S. Childs · Doreen M. Higgins ·
Stephen R. Plymate · Mary L. Disis

Received: 20 May 2013/Accepted: 22 May 2013/Published online: 8 June 2013
© Springer Science+Business Media New York 2013

Abstract Numerous lines of evidence demonstrate that breast cancer is immunogenic; yet, there are few biologically relevant immune targets under investigation restricting the exploration of vaccines to limited breast cancer subtypes. Insulin-like growth factor-I receptor (IGF-IR) is a promising vaccine candidate since it is overexpressed in most breast cancer subtypes, is part of a dominant cancer growth pathway, and has been validated as a therapeutic target. We questioned whether IGF-IR was immunogenic in cancer patients. IGF-IR-specific IgG antibodies were significantly elevated in early-stage breast cancer patients at the time of diagnosis as compared to volunteer donors ($p = 0.04$). Predicted T-helper epitopes, derived from the IGF-IR extracellular and transmembrane domains, elicited a significantly higher incidence of Th2 immunity in breast cancer patients as compared to controls ($p = 0.01$). Moreover, the

magnitude of Th2 immunity was greater in breast cancer patients compared to controls ($p = 0.02$). In contrast, both breast cancer patients and volunteer donors demonstrated a similar incidence of Th1 immunity to IGF-IR domains with the predominant response directed against epitopes in the intracellular domain of the protein. As the incidence of IGF-IR type I immunity was not associated with a breast cancer diagnosis, we questioned whether other factors were contributing to the presence of IGF-IR-specific T-cells in both populations. While age was not associated with Th1 immunity, we observed a significantly greater magnitude of IGF-IR IFN- γ -secreting T-cells in obese subjects as compared to overweight ($p < 0.001$) or healthy-weight ($p = 0.006$) subjects, regardless of breast cancer diagnosis. No significant difference was observed for Th2 incidence or magnitude when stratified by age ($p = 0.174$, $p = 0.966$, respectively) or body mass index ($p = 0.137$, $p = 0.174$, respectively). Our data demonstrate that IGF-IR is a tumor antigen and IGF-IR-specific Th1 immunity may be associated with obesity rather than malignancy.

Electronic supplementary material The online version of this article (doi:[10.1007/s10549-013-2577-z](https://doi.org/10.1007/s10549-013-2577-z)) contains supplementary material, which is available to authorized users.

D. L. Cecil (✉) · E. Gad · J. S. Childs ·
D. M. Higgins · M. L. Disis
Tumor Vaccine Group, Center for Translational Medicine in
Women's Health, University of Washington, 850 Republican
Street, Seattle, WA 98109, USA
e-mail: dcecil@uw.edu

K. H. Park
Division of Oncology/Hematology, Department of Internal
Medicine, Korea University, Seoul, Korea

S. R. Plymate
Department of Medicine, University of Washington, Seattle,
WA, USA

S. R. Plymate
GRECC and Research Service, Department of Veterans Affairs
Medical Center, Seattle, WA, USA

Keywords IGF-IR · Breast cancer antigen · Th1 · Th2 · Obesity

Introduction

Breast cancer has been shown to be immunogenic and clinical trials of cancer vaccines targeting the tumor antigen HER-2/neu (HER2) demonstrate encouraging clinical results in patients with both advanced and early-stage breast cancers [1, 2]. However, there is a paucity of biologically relevant antigens under investigation in breast cancer, and further immune targets need to be identified for additional breast cancer subtypes.

The development of a therapeutic immune response through active immunization requires an immune target that is expressed in a majority of breast cancers. Insulin-like growth factor-I receptor (IGF-IR) is an excellent candidate antigen as it is found upregulated in up to 55 % of breast cancers depending on subtype [3]. Increased IGF-IR signaling is associated with a poor prognosis. In a study of over 400 breast cancer patients, the overall survival at 15 years was significantly increased in the patients whose tumors were negative for the active form of the receptor [4]. Moreover, inactivation of IGF-IR signaling by small molecule inhibitors can result in a 50 % growth inhibition in murine models of human triple-negative breast tumor grafts [5].

We questioned whether IGF-IR was immunogenic in patients with breast cancer by evaluating for the presence of IGF-IR-specific IgG antibodies. As the presence of antibodies is predictive of a preexisting T-cell response [6], we further mapped the phenotype of IGF-IR-specific T-cell immunity across all domains of the growth factor receptor to identify class II epitopes that would be suitable immunogens for the development of a vaccine targeting IGF-IR. Our focus on defining IGF-IR CD4⁺ T-cell epitopes is based on investigations demonstrating that T-cell recognition of cancer occurs via cross-presentation [7]. Vaccines that can elicit Th1 antigen-specific T-cells have the potential for activating antigen-presenting cells in the tumor microenvironment resulting in enhanced cross-priming and the development of epitope spreading to a multitude of tumor antigens [2].

Materials and methods

Human subjects

The use of human subjects was approved by the University of Washington Human Subjects Division. Volunteer control serum from 73 female donors was collected at the Puget Sound Blood Center, Seattle, WA (median age: 51, range 33–73 years). Volunteer controls met all criteria for blood donation. Serum samples from 94 breast cancer patients (100 % Stage I/II; median age 52, range 33–89 years) were obtained from individuals who consented to participate in the FHCRC/UW Breast Specimen Repository and Registry, Peggy Porter, MD, PI (IR file #5306). The serum was collected at the time of diagnosis and prior to definitive surgery. Peripheral blood mononuclear cells (PBMC) from 19 female volunteer controls (median age: 49, range 18–79 years) and 18 breast cancer patients (89 % Stage I/II, 11 % Stage III/IV; median age: 53, range 45–79 years) were collected and cryopreserved as previously described [8]. All breast cancer patients had received definitive treatment for their disease at the time of

collection. Data were available to calculate Body Mass Index (BMI) on 21 individuals.

Analysis of antibody immunity

IgG specific for IGF-IR was assessed by indirect ELISA as previously described with the modification that the Immulon 4HBX microtiter plates (Dynex) were coated overnight with 200 ng/ml human recombinant IGF-IR protein (R&D Systems) in carbonate buffer [9]. Developed plates were read at 450 nm. The OD was calculated as the OD of the protein-coated wells minus the OD of the buffer-coated wells. The data are expressed as µg/ml IGF-IR-specific IgG. The mean and 2 standard deviations of the volunteer control population response, 0.09 µg/ml, defined a level above which a sample was considered positive. Positive and negative samples were assessed by Western blotting [10]. 500 ng of recombinant IGF-IR protein (R&D Systems) was separated on SDS-PAGE gel and probed with anti-IGF-IR polyclonal antibodies (Santa Cruz Biotechnology, Inc.) or experimental sera. Specificity and sensitivity of ELISA were 100 and 75 %, respectively.

Analysis of peptide and protein-specific T-cell responses

Twenty IGF-IR peptides, (21 % of the protein), predicted to promiscuously bind human MHCII, were selected using web-based algorithms as previously described [9]. The peptides were constructed and purified by high-performance liquid chromatography (>90 % pure; Genemed). PBMCs were evaluated by ELISPOT for antigen-specific IFN-γ and IL-10 production. For the IFN-γ ELISPOT, cells were plated at 2 × 10⁵ per well (96-well plate) in medium with 10 µg/ml of the various IGF-IR peptides or HIVp17 (CPC Scientific) [11], PHA (1 µg/ml; Sigma-Aldrich), CEF (2.5 µg/ml; AnaSpec), or medium alone for 7 days at 37 °C in 5 % CO₂. On day 5, recombinant human IL-2 (10 U/ml; Hoffmann-La Roche) was added. A second in vitro stimulation (IVS) was performed on day 8 by adding 2 × 10⁵ peptide-loaded (same concentrations as listed above) autologous irradiated (3000 rads) human PBMCs to the original culture and incubating for 24 h. 96-well nitrocellulose plates (Millipore) were coated with 10 µg/ml anti-human IFN-γ (clone 1-D1K; Mabtech). The washed nitrocellulose plates were blocked with 2 % bovine serum albumin in DPBS followed by 24h incubation with the PBMC culture. After extensive washing, 0.1 µg/ml biotinylated anti-human IFN-γ (clone 7-B6-1; MabTech) was added for 2 h. For the IL-10 ELISPOT [12], an anti-human IL-10-coated (2 µg/ml; BD Biosciences) nitrocellulose 96-well plate was blocked as described above. PBMC concentration and peptide stimulations were as described above, except that PHA was used at 20 µg/ml. After extensive washing, 4 µg/ml

biotinylated anti-human IL-10 (BD Biosciences) was added for 2 h.

Both ELISPOT assays were developed as previously described [9]. Positive responses were defined by a statistically significant difference ($p < 0.05$) between the mean number of spots from five replicates in the experimental wells and the mean number from no antigen control wells. Data are reported as the mean number of spots for each experimental antigen minus the mean number of spots detected in no antigen control wells \pm SEM (corrected spots per well: CSPW) or as mean number of spots.

T-cell lines were generated from volunteer controls demonstrating significant responses to the selected epitopes. PBMCs were thawed, washed, resuspended at $3 \times 10^6/\text{ml}$, and stimulated with 10 $\mu\text{g}/\text{ml}$ of the various IGF-IR peptides. The T-cells were subjected to a second IVS on day 8 and a third IVS on day 16 by adding equivalent numbers of peptide-loaded (10 $\mu\text{g}/\text{ml}$) autologous irradiated (3000 rads) PBMCs to the original culture. Recombinant human IL-12 (10 ng/ml; R&D Systems) and recombinant human IL-2 (10 U/ml) were added on day 5 and day 12, and IL-2 was added alone on days 20, 22, and 24. IFN- γ ELISPOT was performed stimulated with 10 $\mu\text{g}/\text{ml}$ of the original IGF-IR peptides or cos-1 cell lysates transfected with human IGF-IR (IGF-IR) or vector alone (mock) (1 $\mu\text{g}/\text{ml}$), PHA (1 $\mu\text{g}/\text{ml}$), HIVp17 (10 $\mu\text{g}/\text{ml}$), or medium alone (No Ag). Cos-1 cells were transfected with pcDNA-3-hIGF-IR or pcDNA-3 alone (mock) using Polyfect reagent (Qiagen). IGF-IR expression was confirmed by a Western blot probing with anti-IGF-IR polyclonal antibodies (Santa Cruz Biotechnology, Inc.). Cytokine levels were assessed according to the manufacturer's instructions using the appropriate ELISA (eBioscience) on medium collected from the T-cell lines on day 10. Data are expressed as mean $\text{ng}/\text{ml} \pm \text{SD}$ of six separate donor expansions.

Flow cytometry

Receptor expression was documented in the expanded T-cells by adding APC-conjugated anti-human CD4 (clone OKT4, eBioscience) or PE-Cy7-conjugated anti-human CD3 (clone UCYT1, eBioscience). Intracellular expression of FOXP3 was documented after permeabilization and fixation with the FOXP3 Buffer Set (Biolegend) according to the manufacturer's instructions and staining with PE-conjugated anti-human FOXP3 (clone 236A/E7, eBioscience) and anti-human CD4. Flow cytometry was performed on the FACSCanto and data analyzed using FlowJo software (BD Biosciences). Typically, 100,000 cells were collected per sample.

Statistical analysis

The unpaired, two-tailed Student's t test (with Welch's correction when variances were unequal) or Fisher's exact

test was used to evaluate differences. A p value of <0.05 was considered significant (GraphPad Software, Prism v.5.04).

Results

IGF-IR antibodies are significantly elevated in breast cancer patients as compared to volunteer controls

Elevated levels of IGF-IR-specific IgG antibodies were detected in significantly more breast cancer patient sera (9 %, mean, 0.028 $\mu\text{g}/\text{ml}$; range, 0–0.808 $\mu\text{g}/\text{ml}$) than volunteer control sera (1 %, mean, 0.006 $\mu\text{g}/\text{ml}$; range 0–0.364 $\mu\text{g}/\text{ml}$, $p = 0.04$) (Fig. 1a). Antibody responses were confirmed by Western Blot for ELISA positive (Fig. 1b II) and negative donors (Fig. 1b III).

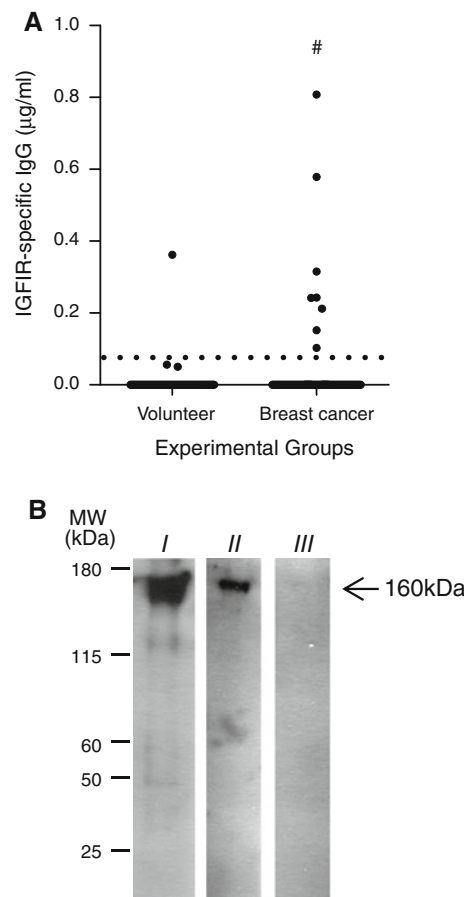


Fig. 1 IGF-IR antibodies are significantly elevated in breast cancer patients as compared to volunteer controls. **a** IGF-IR-specific IgG ($\mu\text{g}/\text{ml}$) (y-axis) for the experimental groups (x-axis). Mean and 2 stand dev of volunteer controls (dotted line), ${}^{\#}p < 0.05$ between groups. **b** Western blot (I) polyclonal anti-IGF-IR Ab of a representative positive (II) and negative (III) ELISA sample. Molecular weight marker (far left). kDa of IGF-IR is marked at 160 kDa

IGF-IR epitopes derived from the extracellular and transmembrane domains of the protein are more likely to induce a higher magnitude Th2 response in breast cancer patients than volunteer controls

Detection of antigen-specific IgG antibodies has been shown to predict the presence of antigen-specific CD4⁺ T-cells [9]. Th2 cells secreting IL-10 will enhance plasma cell function and increase Ig production [13, 14]. We questioned whether IGF-IR-specific IL-10-secreting T-cells could be more readily detected in breast cancer patient PBMCs as compared to volunteer controls. Twenty putative class II epitopes, derived from the IGF-IR protein sequence, were evaluated (Suppl. Table 1). All peptides induced significant IL-10 secretion in some breast cancer patients and volunteer control PBMCs ($p < 0.05$ compared to HIVp17) (Suppl. Fig. 1). Volunteer control donors demonstrated an equivalent incidence of response to epitopes in each IGF-IR domain ($p > 0.05$) (Fig. 2a). Breast cancer patients, however, had a higher incidence of Th2 responses to epitopes in the extracellular (ECD) (35 %, $p = 0.01$) and transmembrane domains (TD) of the protein (53 %, $p < 0.001$) as compared to the intracellular domains (ICD) [31 % kinase domain (KD) and 16 % C-terminal domain (CTD)] (Fig. 2a). In addition, breast cancer patients demonstrated a higher overall incidence of Th2 response to ECD/TD epitopes (88 %) than volunteer controls (56 %, $p = 0.01$).

The breast cancer patients were also more likely to have a higher magnitude Th2 response to the ECD and TD of IGF-IR (mean, 13.1 CSPW; $p = 0.03$ and mean, 26.3 CSPW; $p = 0.02$, respectively) as compared to ICD [KD mean, 11.5 CSPW; CTD mean, 5.4 CSPW (Fig. 2b)]. Furthermore, the breast cancer patients demonstrated an overall greater magnitude of Th2 to TD epitopes than the volunteer controls ($p = 0.02$; mean, 26.3 vs. 13.1 CSPW). This difference was evident even though mitogen-induced IL-10 secretion was decreased in the breast cancer patients

as compared to the controls ($p = 0.047$) (Fig. 2b, Suppl. Fig. 1e). Similar to the incidence of response, the magnitude of the IGF-IR-specific Th2 responses did not differ between domains for the volunteer control population ($p > 0.05$ for all).

IGF-IR epitopes derived from the C-terminal domain induce Th1 immunity at an equivalent incidence, but with a greater magnitude of response in volunteer controls as compared to breast cancer patients

Th1, especially those cells secreting IFN- γ , has been shown to be associated with an anti-tumor response [9]. The presence of IGF-IR-specific antibodies and a predominant Th2 response directed against IGF-IR Th epitopes caused us to question whether IGF-IR-specific Th1 could even be detected in the peripheral blood of breast cancer patients. Th2 inhibits the proliferation of Th1 [15]. All but one IGF-IR epitopes stimulated significant IFN- γ secretion in some breast cancer patients and volunteer control donor PBMCs ($p < 0.05$ compared to HIVp17) (Suppl. Fig. 2). In contrast to IGF-IR-specific Th2 responses, both the breast cancer patients and volunteer control donors had a similar incidence of Th1 immunity to each of the protein domains ($p > 0.05$). Moreover, individuals in both breast cancer (44 %, $p = 0.03$) and volunteer controls (59 %, $p < 0.001$) responded at a greater incidence to epitopes in the CTD than epitopes in the ECD (breast cancer, 29 %; volunteer control, 28 %).

While the magnitude of the IGF-IR-specific Th1 response did not differ between domains for the breast cancer population ($p > 0.05$ for all), volunteer controls were more likely to have higher level Th1 responses to the CTD (mean, 25.4 CSPW) as compared to ECD (mean 13.3 CSPW; $p = 0.01$) (Fig. 3b, Suppl. Fig. 2a,d). Viral (CEF)-specific IFN- γ secretion was equivalent in both populations ($p = 0.512$) (Fig. 3b, Suppl. Fig. 2e).

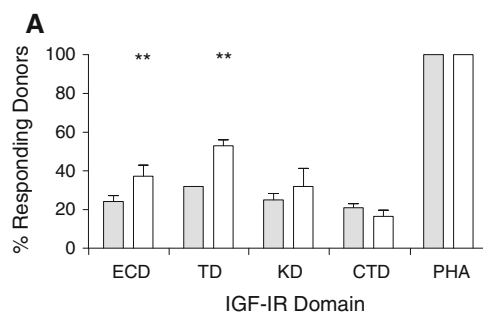
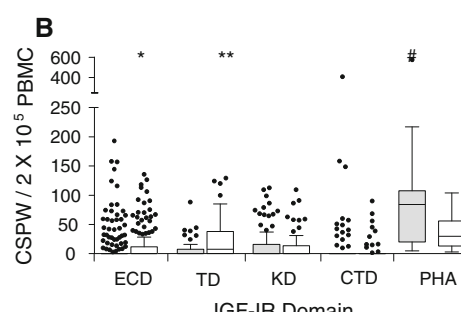


Fig. 2 IGF-IR epitopes derived from the extracellular and transmembrane domains of the protein are more likely to induce a higher magnitude Th2 response in breast cancer patients than volunteer controls. **a** Mean percent IL-10 response to epitopes in the extracellular domain (ECD), transmembrane domain (TD), kinase domain (KD), C-terminal domain (CTD), and PHA for volunteer control



(gray) and breast cancer (white) PBMCs; ** $p < 0.01$ compared to KD and CTD. **b** Corrected spots per well (CSPW) for volunteer control (gray) and breast cancer (white) for epitopes in each domain presented as *interquartile box* plots with Tukey whiskers. Median CSPW are indicated by the horizontal bar; * $p < 0.01$ or ** $p < 0.001$ compared to CTD; # $p < 0.05$ compared to cancer mean CSPW

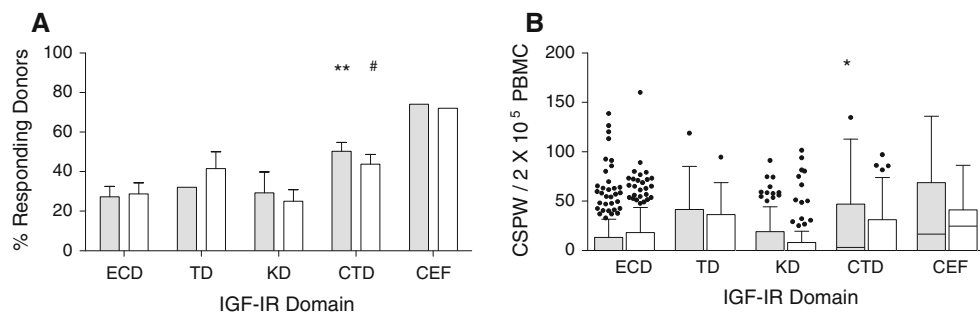


Fig. 3 IGF-IR epitopes derived from the C-terminal domain induce Th1 immunity at an equivalent incidence, but with a greater magnitude response in volunteer controls as compared to breast cancer patients. **a** Mean percent IFN- γ response to epitopes in each domain for volunteer control (gray) and breast cancer (white);

$^{\#}p < 0.05$ or $^{**}p < 0.001$ compared to ECD or KD. **b** CSPW for volunteer control (gray) and breast cancer (white) epitopes in each domain presented as *interquartile box plots* with Tukey whiskers. Median CSPW are indicated by the horizontal bar; $^{*}p < 0.01$ compared to ECD and KD

IGF-IR epitope-specific Th responds to naturally processed and presented IGF-IR protein

We confirmed whether responding sequences were native epitopes of IGF-IR by generating T-cell lines using two peptides randomly chosen from the ECD and one peptide each from the TD, KD, and CTD. The T-cell lines generated (mean, 98.4 %; range 96.2–99 % CD3 $^{+}$ cells) were

predominantly CD4 $^{+}$ (mean, 67.8 %, range 59.8–73.6 %), with CD8 $^{+}$ (mean, 25.5 %; range, 23.3–28.4 %) and CD4 $^{-}$ CD8 $^{-}$ (mean, 1.2 %; range, 0.68–1.88 %) cells. The CD4 $^{+}$ T-cells did not express FOXP3 indicating that the IL-10 secretion observed was via Th2. The T-cells were both IGF-IR peptide- (all $p < 0.05$ compared to HIVp17) and IGF-IR protein-specific (all $p < 0.05$ compared to mock transfectants) (Fig. 4a–c). There was no significant

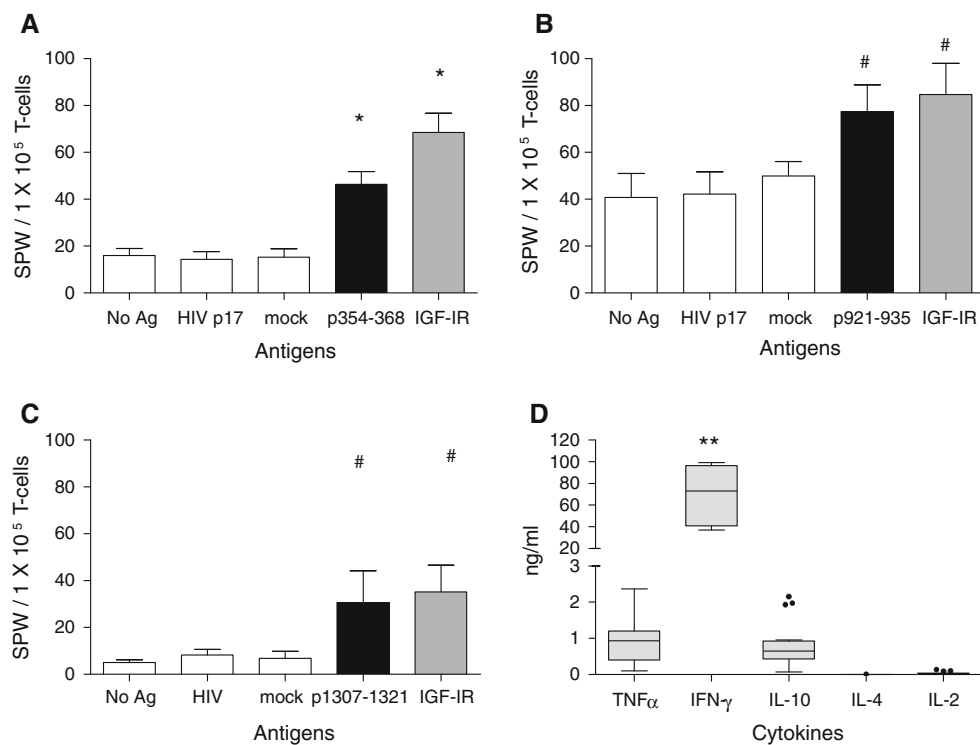


Fig. 4 IGF-IR epitope-specific Th responds to naturally processed IGF-IR protein. **a–c** IFN- γ ELISPOT for IGF-IR-specific T-cell lines. Antigens: none, HIVp17, cos-1 lysate transfected with empty pcDNA (mock) (white), IGF-IR peptides; **a** p354, **b** p921, **c** p1307 (black) and cos-1 cell lysate transfected with pcDNA3 encoding IGF-IR (IGF-IR) (gray). Data are expressed as mean spots per well (SPW) \pm SD;

$^{*}p < 0.05$, $^{**}p < 0.01$. **d** Cytokine secretion from IGF-IR-specific T-cell lines expanded with peptides p354, p545, p921, or p1092 presented as *interquartile box plots* with Tukey whiskers. Median ng/ml is indicated by the horizontal bar from six independent expansions; $^{**}p < 0.001$ compared to TNF α or IL-10 secretion

difference in the level of cytokine secretion induced by any antigen. The T-cells secreted Type I cytokines: TNF α (median, 0.89 ng/ml; range, 0.15–2.2 ng/ml) and IFN- γ (median, 61.8 ng/ml; range, 37.2–97 ng/ml) as well as IL-10 (median, 0.62 ng/ml, range, 0.12–2.02). IFN- γ secretion was significantly greater than TNF α ($p < 0.001$) or IL-10 secretion ($p < 0.001$) (Fig. 4d). Minimal IL-2 (median, 0.01 ng/ml; range, 0–0.11) and IL-4 (median, 0; range, 0–0.003 ng/ml) were detected.

IGF-IR-specific Th1 is found at a greater magnitude in the peripheral blood of obese as compared to healthy-weight and overweight individuals regardless of a breast cancer diagnosis

IGF-IR Th2 immunity appeared to be more prevalent and of higher magnitude in patients with breast cancer inferring the immune response was potentially associated with the diagnosis of malignancy. IGF-IR-specific Th1 immunity had no such association; breast cancer patients and volunteer controls demonstrated an equivalent incidence of IGF-IR-specific Th1 with 49 % of responses (42 % volunteer control and 56 % breast cancer) at the level of a CEF response (Suppl. Fig. 2). For this reason, we explored additional factors, known to potentially impact immunity, as a potential etiology for the presence of detectable IGF-IR-specific Th1 in both populations.

Studies have demonstrated that autoantibody levels and autoreactive lymphocytes increase with age in humans and primates [16–18]; however, there was no significant difference in the incidence ($p = 0.198$) or magnitude ($p = 0.223$) (Fig. 5a) of IGF-IR-specific Th1 between donors below the median age of 42 years compared to those donors above the median age. Obesity is marked by

elevated levels of circulating CD4 $^+$ T-cells secreting IFN- γ [19]. Moreover, IGF-IR has been shown to be aberrantly expressed in obese adipocytes [20]. For this reason, we explored the relationship of the incidence and magnitude of antigen-specific Th1 with BMI. There was no significant difference in the incidence of IGF-IR immunity by BMI ($p > 0.05$ for all groups); however, we observed a significantly greater magnitude of IGF-IR IFN- γ -secreting T-cells in obese subjects than overweight ($p < 0.001$) or healthy-weight ($p = 0.006$) subjects regardless of a breast cancer diagnosis (Fig. 5b). No significant difference was observed in IL-10 incidence or magnitude when stratified by age ($p = 0.174$, $p = 0.966$, respectively) or BMI ($p = 0.137$, $p = 0.174$, respectively).

Discussion

Data presented here demonstrate that IGF-IR is immunogenic. Patients with breast cancer have detectable antibodies directed against IGF-IR. PBMCs from both volunteer controls and breast cancer patients demonstrated evidence of IGF-IR-specific T-cell immunity. In breast cancer patients, Type II immunity was more prevalent and of a higher magnitude directed against the ECD than the intracellular portions of the protein. In contrast, both volunteer controls and breast cancer patients had measurable IGF-IR-specific Th1 directed against the ICD. Of note, the magnitude of IGF-IR-specific Th1 immunity was not associated with a cancer diagnosis, but rather an individual's BMI.

IGF-IR-specific antibodies were found in breast cancer patients. It is known that protein overexpression in breast cancer is directly associated with increasing levels of

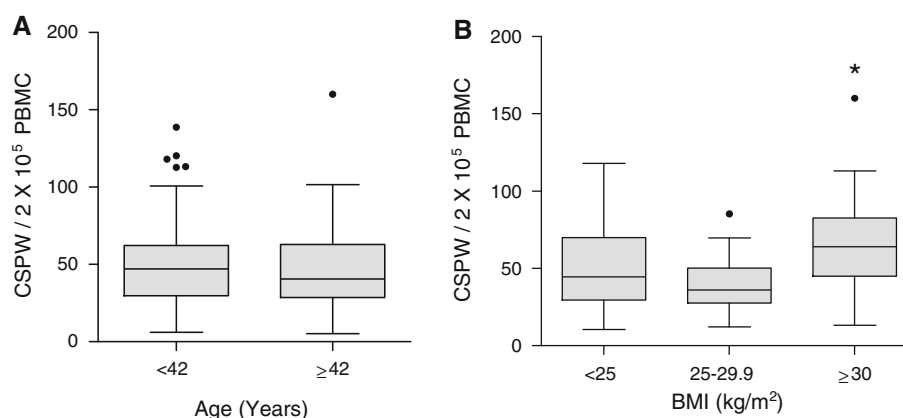


Fig. 5 Higher levels of IGF-IR-specific Th1 are found in the peripheral blood of obese as compared to healthy-weight and overweight individuals regardless of a breast cancer diagnosis. **a** IFN- γ CSPW for all positive responses according to median age (42 years) presented as interquartile box plots with Tukey whiskers.

Median CSPW are indicated by the horizontal bar. **b** IFN- γ CSPW for all positive responses graphed according to BMI. BMI <25 kg/m² (healthy weight); BMI = 25.0–29.9 kg/m² (overweight); BMI ≥30.0 kg/m² (obese). * $p < 0.01$

endogenous antigen-specific antibody immunity. As an example, 82 % (18/22) of breast cancer patients with high HER2 expression levels exhibited HER2-specific antibodies, whereas antigen-specific antibodies were not detected in any patient (0/22) with low protein expression [21]. Upregulation of IGF-IR expression is detected in nearly all subtypes of breast cancer, thus providing a source for increased IGF-IR-specific B-cell activation in patients as compared to volunteer controls [3]. The detection of an IGF-IR-specific humoral response indicates an antigen-specific cellular response as cognate T-cell help is required for immunoglobulin class switching from IgM to IgG [22]. T-cells, particularly Th2, secrete cytokines, such as IL-10 which drive B-cell clonal expansion and antibody production. IL-10 can double B-cell proliferation and increase IgG secretion tenfold in previously activated B-cells [13, 14]. The development of antigen-specific Th2 in breast cancer patients is not unexpected since accumulating evidence demonstrates that the breast tumor microenvironment is dominated by immune suppressive factors, resulting from a chronic inflammatory state [23]. Elevated levels of tumor-infiltrating Th2, producing high levels of IL-4 and IL-13, are found in breast cancer compared to benign tissue [24–26]. Chronic Th2 and B-cell activation can potentiate an immune suppressive tumor microenvironment through cytokine and immunoglobulin production, ultimately resulting in inhibition of the Th1- and CTL-mediated anti-tumor immune response [27, 28].

Th2 was predominantly directed against epitopes in the ECD/TD, suggesting that these sequences may be more tolerogenic. ECD proteins can be shed from the cell surface during homeostatic apoptosis that occurs regularly during development and aging [29, 30]. This exposure may result in more frequent immune presentation of extracellular epitopes leading to tolerance. Studies in animal models of autoimmunity have shown that when intact apoptotic cells are injected, antigen-specific tolerance occurs [31]. In contrast, inoculation with heat-denatured cells elicits an inflammatory immune response and activation of Th1 [32]. The heat-denatured cells release their intracellular components due to rupture of the plasma membrane [33]. The intracellular proteins may be less frequently presented, reducing the opportunity to stimulate tolerance [33]. This notion is consistent with our results demonstrating that IGF-IR-specific Th1 was predominantly directed against epitopes in the ICD.

We detected a similar level of IGF-IR-specific Th1 in volunteer control donors and breast cancer patients, which has been reported for other tumor antigens such as p53 [34]. Studies of p53-specific T-cells demonstrated that these cells were of a memory phenotype, raising the question as to the etiology of antigen exposure in subjects unaffected by cancer. Investigators cited the ubiquitous role of p53 as an oncogene in many cancers and suggested

that Type I p53 precursors could represent a previous exposure to cancer and successful immune surveillance. In our study, we first considered age as an explanation for the elevated IGF-IR-specific Th1. Increased levels of inflammatory cytokines have been shown to positively correlate with aging. In a study examining 73 healthy individuals, those over 60 years exhibit increased levels of IL-1 β , TNF α , and IL-6 compared to younger individuals [35]. Additional investigations have shown that precursor CD4 $^+$ T-cells in aging individuals are predominantly committed to a Th1 phenotype [36]. However, as reported here, the incidence and magnitude of IGF-IR-specific Th1 were not associated with the age of the individual. We explored adiposity as an etiology of the observed immune responses as recent evidence suggests that obesity is also associated with Type I inflammation. Th1 and activated CD8 $^+$ T-cells are the predominant adaptive immune cell infiltrates in adipose tissue [37]. Further, a recent study described a greater number of circulating Th1 in obese individuals compared to overweight and healthy-weight individuals [19]. We found a higher magnitude IGF-IR-specific Th1 immune response in obese subjects compared to overweight and healthy-weight subjects. Why would IGF-IR be a target for the adaptive immune response in obesity? Overexpression of self-antigens during oncogenesis is associated with enhanced immunogenicity, as discussed above [21]. IGF-IR-specific cellular immunity may have been primed by an overexpression of the receptor as a result of increasing adiposity. Studies in humans and animal models of obesity indicate that adipocytes first increase cell size in response to excess energy intake, then increase their number and begin to secrete growth factors which stimulate the proliferation and eventual maturation of pre-adipocytes [38, 39]. Pre-adipocytes isolated from subcutaneous adipose tissue express thirty-fold more IGF-IR protein than mature adipocytes [20]. Collectively, increased antigen exposure and the upregulation of pro-inflammatory cytokines, including IL-12p40 and IL-18, observed in obese adipose tissue may result in the priming of Th1 to adipose-related self-antigens, such as IGF-IR [37].

Evidence of a preexisting Th1 response in breast cancer patients may allow more facile vaccine boosting of that response in patients whose tumors express IGF-IR. Indeed, in a clinical trial targeting p53 in 17 colorectal cancer patients, 33 % of patients with preexisting immunity demonstrated increased levels of antigen-specific T-cells after vaccination, whereas no augmentation of immunity was observed in any patient without preexisting p53-specific T-cells [40]. Our data suggest IGF-IR-specific immunity may also be a marker of inflammatory obesity.

Acknowledgments This work was supported by a grant from the Ovarian Cancer Research Fund, 17624550-36370-A, and a Department of Defense Postdoctoral Fellowship, W81XWH-10-1-0700. MLD is supported by the Athena Distinguished Professorship of Breast Cancer Research.

Conflict of Interest MLD discloses funding received from Seattle Genetics, stock ownership in VentiRx and Epigenomics AG, and a consultant/advisory role at VentiRx and EMD Serono. All other authors disclose no conflict of interest.

Ethical Standards All authors declare that the experiments comply with current U.S. laws.

References

1. Sears AK, Perez SA, Clifton GT, Benavides LC, Gates JD, Clive KS, Holmes JP, Shumway NM, Van Echo DC, Carmichael MG, Ponniah S, Baxevanis CN, Mittendorf EA, Papamichail M, Peoples GE (2011) AE37: a novel T-cell-eliciting vaccine for breast cancer. *Expert Opin Biol Ther* 11:1543–1550
2. Disis ML, Wallace DR, Gooley TA, Dang Y, Slota M, Lu H, Coveler AL, Childs JS, Higgins DM, Fintak PA, dela Rosa C, Tietje K, Link J, Waisman J, Salazar LG (2009) Concurrent trastuzumab and HER2/neu-specific vaccination in patients with metastatic breast cancer. *J Clin Oncol* 27:4685–4692
3. Yerushalmi R, Gelmon KA, Leung S, Gao D, Cheang M, Pollak M, Turashvili G, Gilks BC, Kennecke H (2012) Insulin-like growth factor receptor (IGF-1R) in breast cancer subtypes. *Breast Cancer Res Treat* 132:131–142
4. Law JH, Habibi G, Hu K, Masoudi H, Wang MY, Stratford AL, Park E, Gee JM, Finlay P, Jones HE, Nicholson RI, Carboni J, Gottardis M, Pollak M, Dunn SE (2008) Phosphorylated insulin-like growth factor-i/insulin receptor is present in all breast cancer subtypes and is related to poor survival. *Cancer Res* 68:10238–10246
5. Litzenburger BC, Creighton CJ, Tsimelzon A, Chan BT, Hilsenbeck SG, Wang T, Carboni JM, Gottardis MM, Huang F, Chang JC, Lewis MT, Rimawi MF, Lee AV (2011) High IGF-IR activity in triple-negative breast cancer cell lines and tumorgrafts correlates with sensitivity to anti-IGF-IR therapy. *Clin Cancer Res* 17:2314–2327
6. Lanzavecchia A (1985) Antigen-specific interaction between T and B cells. *Nature* 314:537–539
7. Ma Y, Aymeric L, Locher C, Kroemer G, Zitvogel L (2011) The dendritic cell-tumor cross-talk in cancer. *Curr Opin Immunol* 23:146–152
8. Disis ML, dela Rosa C, Goodell V, Kuan LY, Chang JC, Kuus-Reichel K, Clay TM, Kim Lyerly H, Bhatia S, Ghanekar SA, Maino VC, Maecker HT (2006) Maximizing the retention of antigen specific lymphocyte function after cryopreservation. *J Immunol Methods* 308:13–18
9. Park KH, Gad E, Goodell V, Dang Y, Wild T, Higgins D, Fintak P, Childs J, Dela Rosa C, Disis ML (2008) Insulin-like growth factor-binding protein-2 is a target for the immunomodulation of breast cancer. *Cancer Res* 68:8400–8409
10. Goodell V, McNeel D, Disis ML (2008) His-tag ELISA for the detection of humoral tumor-specific immunity. *BMC Immunol* 9:23
11. Ramduth D, Day CL, Thobakale CF, Mkhwanazi NP, de Pierres C, Reddy S, van der Stok M, Mncube Z, Nair K, Moodley ES, Kaufmann DE, Streeck H, Coovadia HM, Kiepiela P, Goulder PJ, Walker BD (2009) Immunodominant HIV-1 CD4 + T cell epitopes in chronic untreated clade C HIV-1 infection. *PLoS ONE* 4:e5013
12. Guerkov RE, Targoni OS, Kreher CR, Boehm BO, Herrera MT, Tary-Lehmann M, Lehmann PV, Schwander SK (2003) Detection of low-frequency antigen-specific IL-10-producing CD4(+) T cells via ELISPOT in PBMC: cognate vs. nonspecific production of the cytokine. *J Immunol Methods* 279:111–121
13. Fluckiger AC, Garrone P, Durand I, Galizzi JP, Banchereau J (1993) Interleukin 10 (IL-10) upregulates functional high affinity IL-2 receptors on normal and leukemic B lymphocytes. *J Exp Med* 178:1473–1481
14. Roussel F, Garcia E, Defrance T, Peronne C, Vezzio N, Hsu DH, Kastelein R, Moore KW, Banchereau J (1992) Interleukin 10 is a potent growth and differentiation factor for activated human B lymphocytes. *Proc Natl Acad Sci USA* 89:1890–1893
15. O'Garra A (1998) Cytokines induce the development of functionally heterogeneous T helper cell subsets. *Immunity* 8:275–283
16. Ruffatti A, Rossi L, Calligaro A, Del Ross T, Lagni M, Marson P, Todesco S (1990) Autoantibodies of systemic rheumatic diseases in the healthy elderly. *Gerontology* 36:104–111
17. Attanasio R, Brasky KM, Robbins SH, Jayashankar L, Nash RJ, Butler TM (2001) Age-related autoantibody production in a nonhuman primate model. *Clin Exp Immunol* 123:361–365
18. Tachikawa S, Kawamura T, Kawamura H, Kanda Y, Fujii Y, Matsumoto H, Abo T (2008) Appearance of B220low autoantibody-producing B-1 cells at neonatal and older stages in mice. *Clin Exp Immunol* 153:448–455
19. Viardot A, Heilbronn LK, Samocha-Bonet D, Mackay F, Campbell LV, Samaras K (2012) Obesity is associated with activated and insulin resistant immune cells. *Diabetes Metab Res Rev* 28:447–454
20. Bäck KAH (2009) Changes in insulin and IGF-I receptor expression during differentiation of human preadipocytes. *Growth Horm IGF Res* 19:101–111
21. Goodell V, Waisman J, Salazar LG, de la Rosa C, Link J, Coveler AL, Childs JS, Fintak PA, Higgins DM, Disis ML (2008) Level of HER-2/neu protein expression in breast cancer may affect the development of endogenous HER-2/neu-specific immunity. *Mol Cancer Ther* 7:449–454
22. Snapper CM, Kehry MR, Castle BE, Mond JJ (1995) Multivalent, but not divalent, antigen receptor cross-linkers synergize with CD40 ligand for induction of Ig synthesis and class switching in normal murine B cells. A redefinition of the TI-2 vs T cell-dependent antigen dichotomy. *J Immunol* 154:1177–1187
23. DeNardo DG, Coussens LM (2007) Inflammation and breast cancer. Balancing immune response: crosstalk between adaptive and innate immune cells during breast cancer progression. *Breast Cancer Res* 9:212
24. Aspord C, Pedroza-Gonzalez A, Gallegos M, Tindle S, Burton EC, Su D, Marches F, Banchereau J, Palucka AK (2007) Breast cancer instructs dendritic cells to prime interleukin 13-secreting CD4 + T cells that facilitate tumor development. *J Exp Med* 204:1037–1047
25. Pedroza-Gonzalez A, Xu K, Wu TC, Aspord C, Tindle S, Marches F, Gallegos M, Burton EC, Savino D, Hori T, Tanaka Y, Zurawski S, Zurawski G, Bover L, Liu YJ, Banchereau J, Palucka AK (2011) Thymic stromal lymphopoietin fosters human breast tumor growth by promoting type 2 inflammation. *J Exp Med* 208:479–490
26. Caras I, Grigorescu A, Stavaru C, Radu DL, Mogos I, Szegli G, Salageanu A (2004) Evidence for immune defects in breast and lung cancer patients. *Cancer Immunol Immunother* 53:1146–1152
27. Gabitass RF, Annels NE, Stocken DD, Pandha HA, Middleton GW (2011) Elevated myeloid-derived suppressor cells in pancreatic, esophageal and gastric cancer are an independent prognostic factor and are associated with significant elevation of the Th2 cytokine interleukin-13. *Cancer Immunol Immunother* 60:1419–1430
28. Akkoc T, de Koning PJ, Ruckert B, Barlan I, Akdis M, Akdis CA (2008) Increased activation-induced cell death of high IFN-gamma-producing T(H)1 cells as a mechanism of T(H)2 predominance in atopic diseases. *J Allergy Clin Immunol* 121(652–658):e651

29. Elmore S (2007) Apoptosis: a review of programmed cell death. *Toxicol Pathol* 35:495–516
30. Ilan N, Mohsenin A, Cheung L, Madri JA (2001) PECAM-1 shedding during apoptosis generates a membrane-anchored truncated molecule with unique signaling characteristics. *FASEB J* 15:362–372
31. Miyake Y, Asano K, Kaise H, Uemura M, Nakayama M, Tanaka M (2007) Critical role of macrophages in the marginal zone in the suppression of immune responses to apoptotic cell-associated antigens. *J Clin Invest* 117:2268–2278
32. Yoon TJ, Kim JY, Kim H, Hong C, Lee H, Lee CK, Lee KH, Hong S, Park SH (2008) Anti-tumor immunostimulatory effect of heat-killed tumor cells. *Exp Mol Med* 40:130–144
33. Kaczmarek A, Vandenebeele P, Krysko DV (2013) Necroptosis: the release of damage-associated molecular patterns and its physiological relevance. *Immunity* 38:209–223
34. Tsuji T, Matsuzaki J, Ritter E, Miliotto A, Ritter G, Odunsi K, Old LJ, Gnjatic S (2011) Split T cell tolerance against a self/tumor antigen: spontaneous CD4 + but not CD8 + T cell responses against p53 in cancer patients and healthy donors. *PLoS ONE* 6:e23651
35. Alvarez-Rodriguez L, Lopez-Hoyos M, Munoz-Cacho P, Martinez-Taboada VM (2012) Aging is associated with circulating cytokine dysregulation. *Cell Immunol* 273:124–132
36. Sakata-Kaneko S, Wakatsuki Y, Matsunaga Y, Usui T, Kita T (2000) Altered Th1/Th2 commitment in human CD4 + T cells with ageing. *Clin Exp Immunol* 120:267–273
37. Strissel KJ, DeFuria J, Shaul ME, Bennett G, Greenberg AS, Obin MS (2010) T-cell recruitment and Th1 polarization in adipose tissue during diet-induced obesity in C57BL/6 mice. *Obesity (Silver Spring)* 18:1918–1925
38. Marques BG, Hausman DB, Martin RJ (1998) Association of fat cell size and paracrine growth factors in development of hyperplastic obesity. *Am J Physiol* 275:R1898–R1908
39. Hausman DB, DiGirolamo M, Bartness TJ, Hausman GJ, Martin RJ (2001) The biology of white adipocyte proliferation. *Obes Rev* 2:239–254
40. van der Burg SH, Menon AG, Redeker A, Bonnet MC, Drijfhout JW, Tollenaar RA, van de Velde CJ, Moingeon P, Kuppen PJ, Offringa R, Melief CJ (2002) Induction of p53-specific immune responses in colorectal cancer patients receiving a recombinant ALVAC-p53 candidate vaccine. *Clin Cancer Res* 8:1019–1027